Azide−Alkyne "Click" Conjugation of 8-Aza-7-deazaadenine-DNA: Synthesis, Duplex Stability, and Fluorogenic Dye Labeling

Frank Seela* and Suresh S. Pujari

Laboratory of Bioorganic Chemistry and Chemical Biology, Center for Nanotechnology, Heisenbergstraβe 11, 48149 Münster, Germany, and Laboratorium für Organische and Bioorganische Chemie, Institut für Chemie, Universität Osnabrück, Barbarastraβe 7, 49069 Osnabrück, Germany. Received February 19, 2010; Revised Manuscript Received May 31, 2010

The internal dye labeling of DNA by the Huisgen-Meldal-Sharpless "click" reaction is described. Fluorogenic 9-azidomethyl anthracene **2** and 3-azido-7-hydroxycoumarin **3** were employed in the postsynthetic functionalization of oligonucleotides incorporating octa-(1,7)-diynyl-8-aza-7-deaza-2′-deoxyadenosine **1**. Nucleoside **1** was prepared by Sonogashira cross coupling from the corresponding 7-iodo compound, converted into the corresponding phosphoramidite, and oligonucleotides were synthesized. To evaluate the influence of ligands on the oligonucleotide duplex stability, benzyl azide **4** (nonpolar), and 2′,3′-dideoxy azidothymidine **5** (AZT) (polar) were introduced along with the fluorogenic dyes **2** and **3**. DNA duplexes with octa-1,7-diynyl side chains (i.e., containing **1**) are more stable than oligonucleotides containing 8-aza-7-deaza-2′-deoxyadenosine, unveiling that this side chain has steric freedom. A single conjugation by an anthracene residue led to a 9 °C T_m increase of duplex melting. Contrary to 7-deazaadenine dye conjugates, the 8-aza-7-deazaadenine conjugates show virtually no fluorescence quenching, thereby developing almost as strong fluorescence as side chain click derivatives (**32** and **33**) in the absence of 8-aza-7-deazaadenine moiety. Duplexes containing the 8-aza-7-deazaadenine dye conjugate show increased fluorescence over single-stranded DNA. Mismatches with dA, dG, and dC develop reduced fluorescence compared to the fully matched base pair. Molecular dynamics simulations revealed that the bulky dye molecules are accommodated well in duplex DNA.

INTRODUCTION

The visualization of biomolecules provides information about the quantity, localization, and transport in vivo or in vitro (*1*−*3*). Fluorescence spectroscopy is widely used for this purpose, as it is one of the most sensitive spectroscopic techniques (*4*−*6*). As canonical DNA is virtually nonfluorescent, fluorescent or fluorogenic reporter groups are attached to the DNA to enhance its detectibility. Fluorogenic dyes with azido groups can be activated to highly fluorescent molecules by the Cu (I)-catalyzed Huisgen-Meldal-Sharpless azide−alkyne cycloaddition (CuAAC), where the azido group becomes part of a triazole system. Those molecules are used to impart the fluorescence to the nonfluorescent species via a conjugation process (*7*).

The postmodification of DNA by the Cu(I) catalyzed Huisgen 1,3-dipolar cycloaddition reaction (CuAAC) led to consequential improvements in both rate and regioselectivity for introducing reporter molecules in nucleic acids (*8*−*11*). These contributions from Meldal (*12*) and Sharpless (*13*) have changed the perspective of cycloaddition chemistry over the past years. In the quest for near-perfect chemical reactions, the Huisgen-Meldal-Sharpless "click" reaction has emerged as an ideal bioorthogonal protocol for the preparation of rich chemical diversity. As a bioconjugation tool, this concept is extended to life sciences, especially to chemical biology (*14*−*19*) where DNAs or proteins are functionalized for imaging purposes or detection (*20, 21*).

By employing the CuAAC reaction, dye conjugation is performed most efficiently when the ligand is introduced in the major groove of DNA. So, space-demanding molecules do not affect the overall DNA structure. Consequently, pyrimidine nucleobases have been modified at position-5 (*22*−*25*). In purines, the situation is more complex. In principle, the 8-position of adenine or guanine as well as the 6-amino group of adenine can be selected for this purpose (*26*−*28*). (Purine numbering is used throughout the manuscript). However, conjugation at the 8-position interferes with the ribose moiety sterically. So, it is advantageous to use 7-deazapurines in place of purines. They can be efficiently functionalized at that position (*29*) and do not disturb the duplex structure. Our laboratory has had many contributions to this matter over the years (*30*−*32*). Unfortunately, 7-deazapurine pyrrolo[2,3-*d*]pyrimidines can quench the fluorescence of dyes by charge transfer processes (*14, 33*−*37*). This results from the low oxidation potential of pyrrolo[2,3-*d*]pyrimidine nucleosides (*38*), in particular, of 7-deaza-2′-deoxyguanosine and 7-deaza-2′-deoxyadenosine.

Pyrazolo[3,4-*d*]pyrimidines like pyrrolo[2,3-*d*]pyrimidines are ideal shape mimics of purines. They are considered to be much more inert against oxidation thereby leading to a brighter fluorescence of dye molecules covalently linked to DNA (*39*−*43*). Different from purines, and similar to pyrrolo[2,3-*d*]pyrimidines, they can be functionalized at position-7. Consequently, reporter groups of moderate size will be accommodated well in the major groove of B-DNA employing the CuAAC reaction (*14, 18, 19, 37*).

In this manuscript, we report on the synthesis of 8-aza-7-deaza-7-(octa-1,7-diynyl)-2′-deoxyadenosine (**1**). The molecule was converted into the corresponding phosphoramidite **11**, which is further employed in solid-phase oligonucleotide synthesis. The effect of single substitutions as well as of multiple incorporations on the base pairing is evaluated. The ligation with fluorogenic dyes such as 9-azido methyl anthracene **2** (*44*−*46*) or 3-azidocoumarin **3** (*47, 48*) via "click" reaction is studied; benzyl azide **4** and 3′-azido-2′,3′-dideoxythymidine **5** (*49*) were selected to monitor the behavior of less space-demanding residues (Figure 1). The photophysical properties of 8-aza-7-deazapurine conjugates are investigated on the

* Prof. Dr. Frank Seela. Phone: +49(0)251 53406 500. Fax: +49(0)251 53406 857. E-mail: Frank.Seela@uni-osnabrueck.de; Seela@uni-muenster.de. Homepage: www.seela.net.

10.1021/bc100090y
Published on Web 08/03/2010

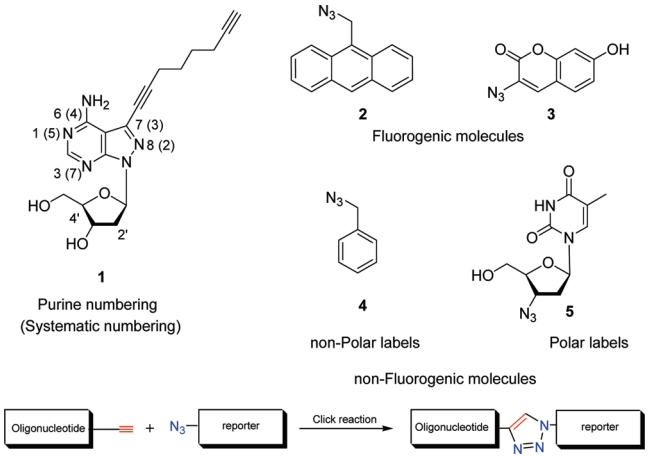

Figure 1. Copper(I)-catalyzed azide−alkyne cycloaddition. Purine numbering; systematic numbering is shown in parentheses.

monomer level, as well as in single-stranded and duplex DNA, and the duplex stability is determined after introducing ligands by "click" conjugation.

EXPERIMENTAL PROCEDURES

General Methods and Materials. All chemicals were purchased from Acros, Fluka, or Sigma-Aldrich (Sigma-Aldrich Chemie GmbH, Deisenhofen, Germany). Solvents were of laboratory grade. Flash column chromatography (FC): silica gel 60 (VWR, Germany) at 0.4 bar; UV spectra: U-3200 spectrometer (Hitachi, Tokyo, Japan). Reversed-phase HPLC was carried out on a 250 × 4 mm RP-18 column (Merck) with a Merck-Hitachi HPLC pump (model L-7100) connected with a variable wavelength monitor (model L-7400). NMR spectra: Avance-DPX-300 spectrometer (Bruker, Rheinstetten, Germany), at 300 MHz for ^{1}H and 75.48 MHz for ^{13}C; δ in ppm relative to Me_4Si as internal standard or external 85% H_3PO_4 for ^{31}P. For NMR spectra recorded in DMSO, the chemical shift of the solvent peak was set to 2.50 ppm for ^{1}H NMR and 39.50 ppm for ^{13}C NMR. MALDI-TOF mass spectra were recorded with Applied Biosystems Voyager DE PRO spectrometer with 3-hydroxypicolinic acid (3-HPA) as a matrix. Elemental analyses were performed by Mikroanalytisches Laboratorium Beller (Göttingen, Germany). The melting temperature curves were measured with a Cary-100 Bio UV−vis spectrophotometer (Varian, Australia) equipped with a Cary thermo-electrical controller. The temperature was measured continuously in the reference cell with a Pt-100 resistor. Fluorescence spectra were recorded in the wavelength range 300−600 nm using the fluorescence spectrophotometer F-2500 (Hitachi, Tokyo, Japan). For solubility reasons, all the 1,2,3-triazole conjugates were dissolved in 0.5 mL DMSO and then diluted with 99.5 mL of methanol. All measurements were performed with identical concentration (9.8×10^{-6} mol/L).

For the synthetic procedure of compound **32**, see the Supporting Information.

1-[2-Deoxy-3,5-di-*O*-(*p*-toluoyl)-β-D-erythropentofuranosyl]-3-(octa-1,7-diynyl)-4-methoxy-1*H*-pyrazolo[3,4-*d*]pyrimidine (7a). A solution of 1-[2-deoxy-3,5-di-*O*-(*p*-toluoyl)-β-D-erythropentofuranosyl]-3-iodo-4-methoxy-1*H*-pyrazolo[3,4-*d*]pyrimidine (**6a**) (*29*) (0.5 g, 0.79 mmol) in dry DMF (7.5 mL) was treated with CuI (0.032 g, 0.16 mmol), $Pd(PPh_3)_4$ (0.096 g, 0.08 mmol), dry Et_3N (0.169 g, 230 μL, 1.67 mmol), and 10 equiv of octa-1,7-diyne (1.03 mL, 7.95 mmol). The reaction mixture which slowly turns to black was stirred under inert atmosphere for 12 h (TLC monitoring). The combined filtrate was evaporated and the oily residue was adsorbed on silica gel and subjected to FC (silica gel, column 15 × 3 cm, eluted with petroleum ether/EtOAc 95:5 → 90:10) affording one main zone. Evaporation of the solvent gave **7a** (0.40 g, 83%) as a yellowish foam. TLC (silica gel, petroleum ether/EtOAC 7.5:2.5). R_f 0.7. UV λ_{max} (MeOH)/nm 275 (ε/dm^3 mol^{-1} cm^{-1} 8300). Anal. ($C_{35}H_{34}N_4O_6$) C, H, N. ^{1}H NMR [DMSO (d_6), 300 MHz]: δ 1.69 (s, 4H, 2 × CH_2), 2.25−2.26 (m, 2H, CH_2), 2.37, 2.39 (2s, 6H, 2 × CH_3), 2.58 (s, 2H, CH_2), 2.79−2.81 (m, 2H, C2′-H_β, C≡CH), 4.11 (s, 3H, OCH_3), 4.44−4.57 (m, 3H, C5′-H, C4′-H), 5.79−5.84 (m, 1H, C3′-H), 6.81−6.85 (t, J = 6.3 Hz, 1H, C1′-H), 7.28−7.36 (m, 4H, Ar−H), 7.87−7.94 (m, 4H, Ar−H), 8.63 (s, 1H, C2−H).

1-[2-Deoxy-β-D-erythropentofuranosyl]-3-(octa-1,7-diynyl)-4-methoxy-1*H*-pyrazolo[3,4-*d*]pyrimidine (7b). As described above for **7a**, with **6b** (0.196 g, 0.5 mmol) in dry DMF (4 mL), CuI (0.019 g, 0.10 mmol), $Pd(PPh_3)_4$ (0.057 g, 0.05 mmol), dry Et_3N (0.01 g, 13 μL, 0.1 mmol), and 10 equiv of octa-1,7-diyne (0.81 mL, 5.02 mmol). FC (silica gel, column 15 × 3 cm, eluted with CH_2Cl_2/MeOH 95:5 → 90:10) affording one main zone. Evaporation of the solvent gave **7b** (0.11 g, 60%) as a colorless solid. TLC (silica gel, CH_2Cl_2/MeOH 9:1). R_f 0.5. UV λ_{max} (MeOH)/nm 233 (ε/dm^3 mol^{-1} cm^{-1} 18 300), 281 (7700). Anal. ($C_{19}H_{22}N_4O_4$) C, H, N. ^{1}H NMR [DMSO (d_6), 300 MHz]: δ 1.67 (s, 4H, 2 × CH_2), 2.25−2.33 (m, 3H, CH_2, C2′-H_α), 2.56 (s, 2H, CH_2), 2.77−2.82 (m, 2H, C2′-H_β, C≡CH), 3.31−3.55 (m, 2H, C5′-H), 3.79−3.85 (m, 1H, C4′-H), 4.11 (s, 3H, OCH_3), 4.42−4.45 (m, 1H, C3′-H), 4.70−4.74 (t, J = 5.7 Hz, 1H, C5′−OH), 5.31−5.32 (d, J = 4.3 Hz, 1H, C3′−OH), 6.61−6.65 (t, J = 6.6 Hz, 1H, C1′-H), 8.63 (s, 1H, C2−H).

1-[2-Deoxy-β-D-erythropentofuranosyl]-3-iodo-1*H*-pyrazolo[3,4-*d*]pyrimidin-4-amine (8). Compound **6a** (*29*) (0.45 g, 0.71 mmol) was stirred at 100 °C for 6 h with a saturated NH_3/MeOH solution (200 cm^3) in an autoclave. The solution was evaporated to dryness and the residue was subjected to FC (column 15 × 3 cm). Evaporation of the solvent afforded compound **8** (0.25 g, 90%) as colorless solid. TLC (silica gel, CH_2Cl_2/MeOH 9:1). R_f 0.6. UV λ_{max} (MeOH)/nm 241 (ε/dm^3 mol^{-1} cm^{-1} 7900), 262 (7300), and 284 (8900). Anal. ($C_{10}H_{12}IN_5O_3$) C, H, N. ^{1}H NMR [DMSO (d_6), 300 MHz]: δ 2.19−2.27 (m, 1H, C2′-H_α), 2.72−2.80 (m, 1H, C2′-H_β), 3.46−3.54 (m, 2H, C5′-H), 3.77−3.82 (m, 1H, C4′-H), 4.38−4.44 (m, 1H, C3′-H), 4.76−4.81 (t, J = 6.0 Hz, 1H, C5′−OH), 5.28−5.29 (d, J = 4.5 Hz, 1H, C3′−OH), 6.47−6.51 (t, J = 6.6 Hz, 1H, C1′-H), 8.22 (s, 1H, C2−H).

1-[2-Deoxy-β-D-erythropentofuranosyl]-3-(octa-1,7-diynyl)-1*H*-pyrazolo[3,4-*d*]pyrimidin-4-amine (1). As described above for **7a**, with **8** (0.398 g, 1.05 mmol) in dry DMF (6 mL), CuI (0.040 g, 0.21 mmol), $Pd(PPh_3)_4$ (0.121 g, 0.10 mmol), dry Et_3N (0.218 g, 2.11 mmol, 0.3 mL), and 8 equiv of octa-1,7-diyne (1.08 mL, 8.4 mmol). FC (silica gel, column 15 × 3 cm, eluted with CH_2Cl_2/MeOH 95:5 → 90:10) afforded one main zone. Evaporation of the solvent gave **1** (0.28 g, 75%) as a colorless foam. TLC (silica gel, CH_2Cl_2/MeOH 9:1). R_f 0.5. UV λ_{max} (MeOH)/nm 249 (ε/dm^3 mol^{-1} cm^{-1} 11 000), 286 (11 300). Anal. ($C_{18}H_{21}N_5O_3$) C, H, N. ^{1}H NMR [DMSO (d_6), 300 MHz]: δ 1.54−1.74 (m, 4H, 2 × CH_2), 2.20−2.27 (m, 3H, CH_2, C2′-H_α), 2.55−2.60 (t, J = 6.9 Hz, 2H, CH_2), 2.72−2.81 (m, 2H, C2′-H_β, C≡CH), 3.27−3.54 (m, 2H, C5′-H), 3.77−3.82 (m, 1H, C4′-H), 4.39−4.42 (m, 1H, C3′-H), 4.75−4.79 (t, J = 6.0 Hz, 1H, C5′−OH), 5.26−5.27 (d, J = 4.5 Hz, 1H, C3′−OH), 6.50−6.54 (t, J = 6.6 Hz, 1H, C1′-H), 8.22 (s, 1H, C2−H).

1-[2-Deoxy-β-D-erythropentofuranosyl]-3-(octa-1,7-diynyl)-4-{[(*N*,*N*-dimethylamino)methylidene)]amino}-1*H*-pyrazolo[3,4-*d*]pyrimidine (9). To a solution of **1** (0.36 g, 0.88 mmol) in MeOH (40 mL) was added *N*,*N*-dimethylformamide dimethyl acetal (3.02 g, 3.36 mL, 25.3 mmol) and the reaction mixture was stirred at rt for 30 min. Then, solvent was evaporated and

residue was subjected to FC (silica gel, column 10 × 4 cm, eluted with CH_2Cl_2/MeOH 97:3 → 90:10). Evaporation of the main zone afforded compound **9** (0.33 g, 79%) as a colorless foam. TLC (CH_2Cl_2/MeOH 9:1). R_f 0.6. UV λ_{max} (MeOH)/nm 322 (ε/dm^3 mol^{-1} cm^{-1} 24 400). Anal. ($C_{21}H_{26}N_6O_3$) C, H, N. ^{1}H NMR [DMSO (d_6), 300 MHz]: δ 1.62−1.67 (m, 4H, 2 × CH_2), 2.21−2.24 (m, 3H, CH_2, C2′-H_α), 2.48−2.55 (m, 2H, CH_2), 2.77−2.81 (m, 2H, C2′-H_β, C≡CH), 3.19, 3.22 (2s, 6H, 2 × CH_3), 3.47−3.52 (m, 1H, C5′-H), 3.79−3.81 (d, J = 3.6 Hz, 1H, C4′-H), 4.41 (s, 1H, C3′-H), 4.77−4.81 (m, 1H, C5′−OH), 5.25−5.26 (d, J = 4.2 Hz, 1H, C3′−OH), 6.55−6.59 (t, J = 6.3 Hz, 1H, C1′-H), 8.43 (s, 1H, C2−H), 8.90 (s, 1H, N=CH).

1-[2-Deoxy-5-*O*-(4,4′-dimethoxytrityl)-β-D-erythropentofuranosyl]-4-{[(*N*,*N*-dimethylamino)methylidene]amino}-3-(octa-1,7-diynyl)-1*H*-pyrazolo[3,4-*d*]pyrimidine (10). Compound **9** (0.59 g, 1.44 mmol) was dried by repeated coevaporation with dry pyridine (3 × 5 mL). The residue was dissolved in dry pyridine and stirred with 4,4′-dimethoxytrityl chloride (0.58 g, 1.72 mmol) at rt for 6 h. After completion of the reaction (monitored by TLC), methanol (6 mL) was added to the reaction mixture, and stirring was continued for another half an hour. The reaction mixture was evaporated to dryness under reduced pressure and the remaining residue was dissolved in dichloromethane (50 mL) and washed with 5% aq $NaHCO_3$ solution (2 × 250 mL) and water (80 mL). The organic layer was dried over Na_2SO_4, the solvent was evaporated under reduced pressure, and the residue was subjected to FC (silica gel, column 10 × 4 cm, eluted with CH_2Cl_2/acetone 95:5 → 90:10). Evaporation of the main zone afforded **10** (0.72 g, 70%) as a colorless foam. TLC (silica gel, CH_2Cl_2/MeOH 9:1). R_f 0.7. UV λ_{max} (MeOH)/nm 225 (ε/dm^3 mol^{-1} cm^{-1} 41 800), 320 (24 900). Anal. ($C_{42}H_{44}N_6O_5$) C, H, N. ^{1}H NMR [DMSO (d_6), 300 MHz]: δ 1.58−1.69 (m, 4H, 2 × CH_2), 2.17−2.22 (m, 2H, CH_2), 2.28−2.32 (m, 1H, CH), 2.49−2.54 (m, 2H, CH_2), 2.77−2.88 (m, 2H, C≡CH, C2′-H_β), 3.00−3.09 (m, 2H, C5′-H), 3.19−3.22 (s, 6H, 2 × CH_3), 3.69 (s, 6H, 2 × OCH_3), 3.90−3.93 (m, 1H, C4′-H), 4.51−4.52 (m, 1H, C3′-H), 5.30−5.32 (d, J = 4.8 Hz, 1H, C3′−OH), 6.58−6.62 (m, 1H, C1′-H), 6.70−6.77 (m, 4H, Ar−H), 7.14−7.21 (m, 7H, Ar−H), 7.29−7.31 (m, 2H, Ar−H), 8.46 (s, 1H, C2−H), 8.90 (s, 1H, N=CH).

1-[2-Deoxy-5-*O*-(4,4′-dimethoxytrityl)-β-D-erythropentofuranosyl]-4-{[(*N*,*N*-dimethylamino)methylidene]amino}-3-(octa-1,7-diynyl)-1*H*-pyrazolo[3,4-*d*]pyrimidin-3′-(2-cyanoethyl)-*N*,*N*-diisopropylphosphoramidite (11). A solution of **10** (0.12 g, 0.16 mmol) in dry CH_2Cl_2 (10 mL) was stirred with (i-Pr)$_2$NEt (57 μL, 0.33 mmol) at rt. Then, 2-cyanoethyl diisopropylphosphoramidochloridite (75 μL, 0.33 mmol) was added, and the reaction mixture was stirred for 30 min. After completion of the reaction (monitored by TLC), the reaction mixture was diluted with CH_2Cl_2 (30 mL) and was poured into 5% $NaHCO_3$ solution (30 mL) and extracted with CH_2Cl_2 (3 × 30 mL). The combined organic phases were dried over Na_2SO_4, and the solvent was evaporated. The residual foam was applied to FC (silica gel, column 8 × 3 cm, eluted with CH_2Cl_2/acetone 100:0 → 95:5). Evaporation of the main zone afforded **11** (0.11 g, 74%) as a colorless foam. TLC (silica gel, CH_2Cl_2/acetone 9:1). R_f 0.7. ^{31}P NMR ($CDCl_3$, 121 MHz): 148.26, 148.39.

4-Amino-1-[2-deoxy-β-D-erythropentofuranosyl]-3-[(methylanthracene-1′,2′,3′-triazol-4′-yl)hexylidyne]-1*H*-pyrazolo[3,4-*d*]pyrimidine (12). To a solution of **1** (0.15 g, 0.42 mmol) and anthracene azide **2** (0.12 g, 0.50 mmol) in THF/H_2O/t-BuOH, (3:1:1; 5 mL) was added sodium ascorbate (419 μL, 0.41 mmol) of a freshly prepared 1 M solution in water, followed by the addition of copper(II) sulfate pentahydrate 7.5% in water (362 μL, 0.10 mmol). The emulsion was stirred for 12 h at rt, and the solution was evaporated and applied to FC (silica gel, column 10 × 3 cm, CH_2Cl_2/MeOH 88:12). From the main zone, compound **12** (0.21 g, 85%) was isolated as a yellowish foam. TLC (silica gel, CH_2Cl_2/MeOH 8:2). R_f 0.5. UV λ_{max} (MeOH)/nm 348 (ε/dm^3 mol^{-1} cm^{-1} 5600), 365 (7600), 386 (6900). Anal. ($C_{33}H_{32}N_8O_3$) C, H, N. ^{1}H NMR [DMSO (d_6), 300 MHz]: δ 1.13−1.19 (m, 2H, CH_2), 1.55−1.65 (m, 4H, 2 × CH_2), 2.19−2.27 (m, 1H, C2′-H_α), 2.48−2.54 (m, 2H, CH_2), 2.73−2.78 (m, 1H, C2′-H_β), 3.79−3.84 (m, 1H, C4′-H), 4.40 (br s, 1H, C3′-H), 4.81 (br s, 1H, C5′−OH), 5.29−5.34 (m, 1H, C3′−OH), 6.50−6.54 (m, 1H, C1′-H), 6.58 (s, 2H, CH_2), 7.53−7.66 (m, 4H, Ar−H), 7.71 (s, 1H, triazole-H), 8.13 (s, 1H, Ar−H), 8.16 (s, 1H, Ar−H), 8.22 (s, 1H, C2−H), 8.56 (s, 1H, Ar−H), 8.60 (s, 1H, Ar−H), 8.72 (s, 1H, Ar−H). ESI-TOF: [M + Na]$^+$ calcd 611.66. Found 611.20.

4-Amino-1-[2-deoxy-β-D-erythropentofuranosyl]-3-[(7-hydroxycoumarin-1′,2′,3′-triazol-4′-yl)hexylidyne]-1*H*-pyrazolo[3,4-*d*]pyrimidine (13). As described above for **12**. A solution of **1** (0.100 g, 0.28 mmol) and 3-azido-7-hydroxy-coumarin **3** (0.068 g, 0.43 mmol) in THF/H_2O/t-BuOH (3:1:1, 4 mL), sodium ascorbate (280 μL, 0.28 mmol), copper(II) sulfate pentahydrate 7.5% in water (242 μL, 0.07 mmol). FC (silica gel, column 10 × 3 cm, CH_2Cl_2/MeOH 88:12) afforded **13** (0.135 g, 86%) as a yellowish solid. TLC (silica gel, CH_2Cl_2/MeOH 8:2). R_f 0.6. UV λ_{max} (MeOH)/nm 287 (ε/dm^3 mol^{-1} cm^{-1} 15 200), 346 (19 500). ^{1}H NMR [DMSO (d_6), 300 MHz]: δ 1.65−1.80 (m, 4H, 2 × CH_2), 2.17−2.25 (m, 1H, C2′-H_α), 2.58−2.63 (m, 2H, CH_2), 2.73−2.79 (m, 3H, C2′-H_β, CH_2), 3.47−3.52 (m, 2H, C5′-H), 3.76−3.79 (m, 1H, C4′-H), 4.39 (br s, 1H, C3′-H), 4.78 (br s, 1H, C5′−OH), 5.27 (br s, 1H, C3′−OH), 6.48−6.53 (t, J = 6.3 Hz, 1H, C1′-H), 6.83 (s, 1H, C7″-H), 6.87−6.91 (d, J = 3.0 Hz, 1H, C9″-H), 7.70−7.73 (d, J = 8.7 Hz, 1H, triazole-H), 8.21 (s, 1H, C6″-H), 8.33 (s, 1H, C2−H), 8.55 (s, 1H, C4″-H). ESI-TOF: [M + Na]$^+$ calcd 581.55. Found 581.18.

4-Amino-1-[2-deoxy-β-D-erythropentofuranosyl]-3-{[(1,2,3,4-tetrahydro-5-methyl-2,4-dioxopyrimidin-1-yl)furan-3-yl]-(1,2,3-triazol-4′-yl)hexylidyne}-1*H*-pyrazolo[3,4-*d*]pyrimidine (14). As described above for **12**. A solution of **1** (0.05 g, 0.14 mmol) and AZT **5** (0.045 g, 0.16 mmol) in THF/H_2O/t-BuOH, (3:1:1, 3 mL), sodium ascorbate (150 μL, 0.15 mmol), copper(II) sulfate pentahydrate 7.5% in water (130 μL, 0.03 mmol). FC (silica gel, column 10 × 3 cm, CH_2Cl_2/MeOH 80:20) afforded **14** (0.071 g, 81%) as a colorless solid. TLC (silica gel, CH_2Cl_2/MeOH 7:3). R_f 0.2. UV λ_{max} (MeOH)/nm 269 (ε/dm^3 mol^{-1} cm^{-1} 17 900). Anal. ($C_{28}H_{34}N_{10}O_7$) C, H, N. ^{1}H NMR [DMSO (d_6), 300 MHz]: δ 1.66−1.76 (m, 4H, CH_2), 1.80 (s, 3H, CH_3), 2.08 (s, 3H, CH_3), 2.13−2.44 (m, 1H, C2′-H_α), 2.57−2.62 (m, 3H, CH_2, C2′-H_β), 2.66−2.80 (m, 4H, CH_2), 3.47−3.52 (m, 2H, C5′-H), 3.57−3.67 (m, 2H, C5′-H), 3.70−3.82 (m, 2H, C4′-H), 4.18−4.19 (m, 1H, C3′-H), 4.39−4.42 (m, 1H, C3′-H), 4.72−4.77 (m, 1H, 3′−OH), 5.27−5.31 (m, 2H, 5′−OH), 6.38−6.42 (t, J = 6.6 Hz, 1H, C1′-H), 6.49−6.54 (t, J = 6.3 Hz, 1H, C1′-H), 7.81 (s, 1H, triazole-H), 8.06 (s, 1H, C2−H), 8.22 (s, 1H, C2−H), 11.36 (s, 1H, NH). ESI-TOF: [M + Na]$^+$ calcd 645.63. Found 645.25.

4-Amino-1-[2-deoxy-β-D-erythropentofuranosyl]-3-[(benzyl-1′,2′,3′-triazol-4′-yl)hexylidyne]-1*H*-pyrazolo[3,4-*d*]pyrimidine (15). As described above for **12**. A solution of **1** (0.100 g, 0.28 mmol) and benzyl azide **4** (0.045 g, 0.33 mmol) in THF/H_2O/t-BuOH, (3:1:1, 5 mL), sodium ascorbate (280 μL, 0.28 mmol), copper(II) sulfate pentahydrate 7.5% in water (242 μL, 0.07 mmol). FC (silica gel, column 10 × 3 cm, CH_2Cl_2/MeOH 90:10) afforded **15** (0.124 g, 90%) as a colorless solid. TLC (silica gel, CH_2Cl_2/MeOH 8:2). R_f 0.5. UV λ_{max} (MeOH)/nm 249 (ε/dm^3 mol^{-1} cm^{-1} 10 500), 287 (10 100). Anal. ($C_{25}H_{28}N_8O_3$) C, H, N. ^{1}H NMR [DMSO (d_6), 300 MHz]: δ 1.60−1.73 (m, 4H, 2 × CH_2), 2.22−2.25 (m, 1H, C2′-H_α),

2.55−2.60 (t, J = 6.9 Hz, 2H, CH_2), 2.64−2.68 (t, J = 7.2 Hz, 2H, CH_2), 2.71−2.80 (m, 1H, C2′-H_β), 3.47 (s, 1H, C5′-H), 3.78−3.82 (m, 1H, C4′-H), 4.40 (br s, 1H, C3′-H), 4.78 (br s, 1H, C5′−OH), 5.28 (br s, 1H, C3′−OH), 5.54 (s, 2H, CH_2), 6.50−6.54 (t, J = 6.3 Hz, 1H, C1′-H), 7.26−7.35 (m, 4H, Ar−H), 7.91 (s, 1H, triazole-H), 8.22 (s, 1H, C2−H). ESI-TOF: $[M + H]^+$ calcd 489.54. Found 489.23.

4-Amino-7-[2-deoxy-β-D-erythropentofuranosyl]-5-[(methylanthracen-1′,2′,3′-triazol-4′-yl)hexylidyne]-7*H*-pyrrolo[2,3-*d*]pyrimidine (16). As described above for **12**. A solution of 1-(2-deoxy-β-D-erythropentofuranosyl)-5-(octa-1,7-diynyl)-1*H*-pyrrolo[2,3-*d*]pyrimidin-4-amine (*14*) (0.100 g, 0.28 mmol) and anthracence azide **2** (0.079 g, 0.33 mmol) in THF/H_2O/*t*-BuOH, (3:1:1, 4 mL), sodium ascorbate (280 μL, 0.28 mmol), copper(II) sulfate pentahydrate 7.5% in water (242 μL, 0.073 mmol). FC (silica gel, column 10 × 3 cm, CH_2Cl_2/MeOH 88:12) afforded **16** (0.13 g, 78%) as a yellowish solid. TLC (silica gel, CH_2Cl_2/MeOH 8:2). R_f 0.5. UV λ_{max} (MeOH)/nm 279 (ε/dm^3 mol^{-1} cm^{-1} 17 400), 348 (8300), 366 (12 300), 386 (11 300). Anal. ($C_{34}H_{33}N_7O_3$) C, H, N. ^{1}H NMR [DMSO (d_6), 300 MHz]: δ 1.48−1.65 (m, 4H, 2 × CH_2), 2.17−2.20 (m, 1H, C2′-H_α), 2.40−2.45 (m, 2H, CH_2), 2.49−2.56 (m, 3H, C2′-H_β, CH_2), 3.52−3.55 (m, 2H, C5′-H), 3.80−3.84 (m, 1H, C4′-H), 4.33 (s, 1H, C3′-H), 5.08 (br s, 1H, C5′−OH), 5.27 (br s, 1H, C3′−OH), 6.44−6.49 (m, 3H, CH_2, C1′-H), 6.58 (s, 2H, Ar−H, C8−H), 7.52−7.65 (m, 4H, Ar−H), 7.70 (s, 1H, triazole-H), 8.13 (s, 1H, Ar−H), 8.16 (s, 1H, Ar−H), 8.57 (s, 1H, C2−H), 8.59 (s, 1H, Ar−H), 8.71 (s, 1H, Ar−H), 8.70 (s, 1H, Ar−H). ESI-TOF: $[M + Na]^+$ calcd 610.67. Found 611.25.

Synthesis, Purification, and Characterization of Oligonucleotides 17−26. The syntheses of oligonucleotides were performed on a DNA synthesizer, model 392−08 (Applied Biosystems, Weiterstadt, Germany), at 1 μmol scale using the phosphoramidite **11** following the synthesis protocol for 3′-*O*-(2-cyanoethyl)phosphoramidites. After cleavage from the solid support, the oligonucleotides were deprotected in 25% aqueous ammonia solution for 16 h at 60 °C. The purification of the "trityl-on" oligonucleotides was carried out on reversed-phase HPLC using the following gradient system at 260 nm: (A = MeCN, B = 0.1 M (Et_3NH)OAc (pH 7.0)/MeCN, 95:5): 0−3 min 10−15% A in B, 3−15 min 15 −50% A in B, and 15−20 min 50−10% A in B; flow rate 1.0 mL/min. The purified "trityl-on" oligonucleotides were treated with 2.5% $CHCl_2COOH$/CH_2Cl_2 for 5 min at 0 °C to remove the 4,4′-dimethoxytrityl residues. The detritylated oligomers were purified again by reversed-phase HPLC (gradient: 0−20 min 0−20% A in B; 20−25 min, 20% A in B, 25−30 min 20−0% A in B, flow rate 1.0 mL/min). The oligonucleotides were desalted on column (RP-18) using water for elution of salt, while the oligonucleotides were eluted with H_2O/MeOH (2:3). The oligonucleotides were lyophilized on a Speed-Vac evaporator to yield colorless solids which were frozen at −24 °C. The enzymatic hydrolysis of oligonucleotide **19** was performed using snake-venom phosphodiesterase (EC 3.1.15.1, *Crotallus adamanteus*) and alkaline phosphatase (EC 3.1.3.1, *Escherichia coli* from Roche Diagnostics GmbH, Germany) in 0.1 M Tris HCl buffer (pH 8.5) at 37 °C, which was analyzed by reversed-phase HPLC (RP-18) showing the peaks of the modified and unmodified nucleosides. The extinction coefficients ε_{260} of the nucleosides: dA 15400, dG 11700, dT 8800, dC 7300, and **1** 8500. The molecular masses of oligonucleotides **17−30** were determined by MALDI-TOF mass spectrometry in the linear negative mode (Supporting Information).

Click Conjugation of Oligonucleotide 19 with Azides 2−5 to Yield Oligonucleotide Conjugates 27−30. To the single-stranded oligonucleotide **19** (5 A_{260} units), a 1:1 $CuSO_4$−TBTA ligand complex (50 μL of a 20 mM stock solution in *t*-BuOH/H_2O 1:9), tris(carboxyethyl)phosphine (TCEP; 50 μL of a 20 mM stock solution in water), respective azide (50 μL of a 20 mM stock solution in dioxane/H_2O 1:1), sodium bicarbonate (50 μL of a 20 mM aq solution), and 35 μL DMSO were added and stirred at room temperature for 12 h. The reaction mixture was concentrated in a speed vac and dissolved in 0.5 mL bidistilled water and centrifuged for 20 min at 14 000 rpm. The supernatant solution was collected and further purified by reversed-phase HPLC. Oligonucleotides **28−30** were purified by the following gradient [0−20 min 0−20% A in B; 20−25 min 20% A in B, 25−30 min 20−0% A in B, flow rate 1.0 mL/min] to give the "click" product. The oligonucleotide **27** was purified by reversed-phase HPLC using following gradient system [A = MeCN, B = 0.1 M (Et_3NH)OAc (pH 7.0)/MeCN, 95: 5): 0−3 min 10−15% A in B, 3−15 min 15 −50% A in B, and 15−20 min 50−10% A in B; flow rate 1.0 mL/min]. The molecular masses of oligonucleotides **27−30** were determined by MALDI-TOF mass spectrometry in the linear negative mode (Supporting Information).

RESULTS AND DISCUSSION

Synthesis and Characterization of Monomers. The synthesis and behavior of oligonucleotides incorporating 7-deaza-7-(octa-1,7-diynyl)-2′-deoxyadenosine (*14*) was reported by our laboratory. Now, oligonucleotides containing 8-aza-7-deaza-7-(octa-1,7-diynyl)-2′-deoxyadenosine **1** were synthesized. For the synthesis of nucleoside **1**, two alternative routes were employed: (a) Sonogashira cross coupling was performed on the sugar-protected 6-methoxy nucleoside **6a** (*29*) with octa-1,7-diyne to yield **7a** in 83%. This was deprotected with sodium methoxide in methanol to give **7b** (60%) (*29*). Amination in saturated methanolic ammonia (steel vessel, 100 °C) resulted in **1** in 89%. (b) Deprotection of the methoxy compound **6a** in methanolic ammonia to **6b** under simultaneous amination gave **8** (90%). Sonogashira cross coupling on **8** with octa-1,7-diyne gave **1** in 75% yield (Scheme 1). The 6-methoxy compound **6a** is a ubiquitous precursor for a series of 6-substituted nucleosides.

Next, the phosphoramidite building block **11** was prepared from the alkynylated nucleoside **1** (Scheme 2). Amino group protection was performed on **1** with the *N,N*-dimethylaminomethylidene group to afford the intermediate **9** in 79% yield. This

Scheme 1. Synthesis of Nucleoside 1 and Related Derivatives[a]

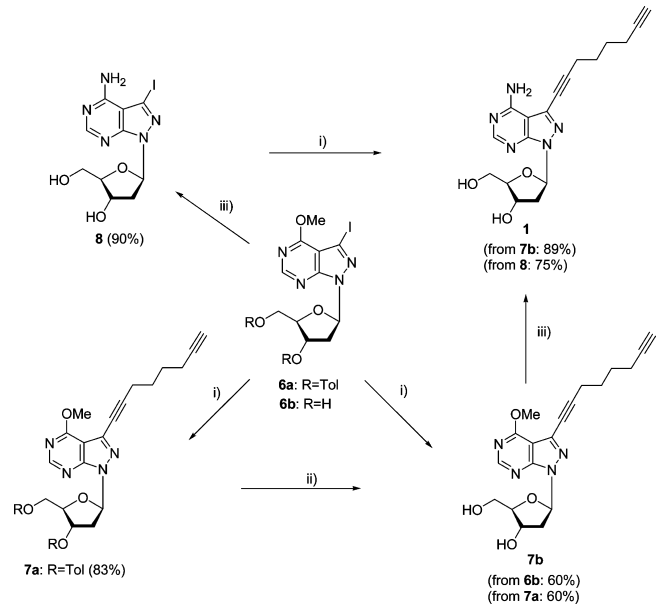

[a] (i) Octa-1,7-diyne, [$Pd^0[P(Ph_3)_4]$], CuI, DMF, Et_3N, rt, 12 h; (ii) NaOMe/MeOH, rt, 8 h (*29*); (iii) NH_3/MeOH, autoclave 100 °C, 6 h.

Scheme 2. Synthesis of Phosphoramidite Building Block 11[a]

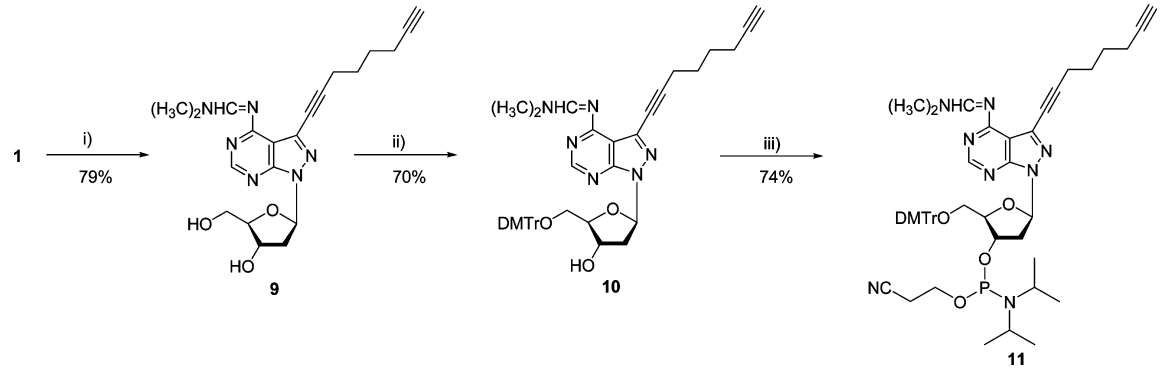

[a] (i) *N,N*-Dimethylformamide dimethylacetal, MeOH, rt, 30 min; (ii) 4,4′-dimethoxytriphenylmethyl chloride, anhydrous pyridine, rt, 6 h; (iii) 2-cyanoethyl-*N,N* diisopropylchlorophosphoramidite, anhydrous CH_2Cl_2, $(i\text{-Pr})_2EtN$, rt, 30 min.

Table 1. ^{13}C NMR Chemical Shifts of the 8-Aza-7-deaza-2′-deoxyadenosine Derivatives[a]

	C(2)[b] C(6)[c]	C(4)[b] C(7a)[c]	C(5)[b] C(3a)[c]	C(6)[b] C(4)[c]	C(7)[b] C(3)[c]	C≡C	CH_2	CH_3/N=CH	C(1′)	C(2′)	C(3′)	C(4′)	C(5′)
1	156.6	153.6	100.8	157.8	127.2	96.4	27.3	--	84.0	37.9	70.9	87.7	62.3
						84.3	26.7						
						72.2	18.4						
						71.4	17.2						
7a	156.2	154.9	103.3	163.5	127.8	95.2	27.0	54.6	84.2	35.3	74.6	81.6	63.8
						84.3	26.8	21.2					
						72.5	18.2						
						71.4	17.3						
7b	156.0	154.7	103.2	163.5	127.4	95.1	27.1	54.5	84.4	37.9	70.9	87.8	62.3
						86.9	26.8						
						72.6	18.2						
						71.4	17.3						
8	156.2	153.9	103.4	157.6	91.2	--	--	--	83.9	37.8	70.9	87.6	62.3
9	155.8	154.4	107.7	162.2	128.9	93.8	27.3	34.7	83.9	37.9	70.9	87.7	62.3
						84.2	27.0	40.7					
						73.6	18.3	157.7					
						71.4	17.2						
10	155.8	154.5	107.8	162.2	128.9	93.6	27.3	34.7	83.7	38.0	70.5	85.3	64.1
						84.2	27.1	40.7					
						73.8	18.4	157.9					
						71.4	17.3						

[a] Measured in DMSO(d_6) at 298 K. All ^{13}C chemical shifts were unambiguously assigned by gated-decoupled $^1H-^{13}C$ NMR spectra. For $^1H-^{13}C$ coupling constants, see Table S1, Supporting Information. [b] Purine numbering. [c] Systematic numbering.

protected nucleoside was converted to the respective 5′-*O*-DMT-derivative under standard reaction conditions, to yield **10** in 70%, and further phosphitylation gave the corresponding phosphoramidite **11** in 74% (Scheme 2).

All the synthesized compounds were characterized by either elemental analyses or molecular mass, ^1H and ^{13}C NMR, as well as $^1H-^{13}C$ NMR gated decoupled spectra (for $^1H-^{13}C$ NMR coupling constants, see Supporting Information). The ^{13}C NMR chemical shifts are listed in Table 1. Terminal triple bonds are not affected by the Pd-assisted Sonogashira cross coupling by the competitive reactions like allene formation, as the table indicates four signals of methylene carbons (27.3, 26.7, 18.4, and 17.2 ppm) and four signals for the triple bond carbons (**1**: 71.4, 72.2, 84.3, 96.4 ppm; Table 1) and even confirmed by inverted signals of distortionless enhancement by polarization transfer (DEPT-135) spectra.

Synthesis, Characterization, and Duplex Stability of Oligonucleotides Containing Nucleoside 1. To evaluate the potential of the base modification on the duplex stability and fluorescence behavior, oligonucleotides were prepared by solid-phase synthesis using the phosphoramidite **11** as building block. The synthesis was performed in a 1 μmol scale. The coupling yields were always higher than 95%. Deprotection of the oligonucleotides was performed in 25% aqueous NH_3 at 60 °C for 16 h. The oligonucleotides were purified by both "trityl on" and "trityl off" modus by reversed-phase HPLC. (For details, see Experimental Procedures.) The base composition of the oligonucleotides was determined by tandem enzymatic hydrolysis with snake-venom phosphodiesterase followed by alkaline phosphatase in 0.1 M Tris-HCl buffer (pH 8.5) at 37 °C (Supporting Information). Molecular masses were determined by MALDI-TOF mass spectrometry, which were found in agreement with calculated values.

Earlier, we reported on the influence of substituents on the duplex stability and base pairing properties of 5-substituted pyrimidines and 7-substituted-7-deazapurines containing alkynyl side chains (*14, 50*). It was inferred that nucleosides having halogen and propynyl side chains attached to the 7-position of pyrrolo[2,3-*d*]pyrimidines or pyrazolo[3,4-*d*]pyrimidines are accommodated well in the major groove of DNA, thus rendering thermal stability to the duplexes (*51*−*54*). Further studies showed that 7-alkynyl chains of length three to six carbon atoms and one triple bond led to stabilization of DNA duplex while longer chains show a negative effect on the stability because of the increased hydrophobic character, which arises due to the alkynyl chain (*51*−*54*). On the other hand, we demonstrated that long chain linkers with terminal triple bonds such as octa-1,7-diynyl or propargyl ether show a positive influence on the duplex stability similar to that of a propynyl residue (*14, 50*).

Now, the duplex stability of oligonucleotides is studied to determine the influence of modification by nucleoside **1** as surrogate of 2′-deoxyadenosine. The oligonucleotide duplex 5′-

Table 2. T_m Values and Thermodynamic Data of Oligonucleotide Duplexes Containing Nucleoside 1

duplexes	T_m [a] [°C]	ΔT_m [b] [°C]	ΔH° [c] [kcal/mol]	ΔS° [cal/(mol K)]	ΔG°_{310} [kcal/mol]
5′-d(TAG GTC AAT ACT) (**17**)					
3′-d(ATC CAG TTA TGA) (**18**)	50	--	−89	−249	−11.6
5′-d(TAG GTC **1**AT ACT) (**19**)					
3′-d(ATC CAG TTA TGA) (**18**)	51	+1	−83	−231	−11.6
5′-d(TAG GTC **11**T ACT) (**20**)					
3′-d(ATC CAG TTA TGA) (**18**)	54	+4	−84	−232	−12.3
5′-d(T**1**G GTC **11**T **1**CT) (**21**)					
3′-d(ATC CAG TTA TGA) (**18**)	56	+6	−92	−256	−13.2
5′-d(TAG GTC AAT ACT) (**17**)					
3′-d(ATC CAG TTA TG**1**) (**22**)	52	+2	−85	−238	−11.8
5′-d(TAG GTC AAT ACT) (**17**)					
3′-d(ATC C**1**G TT**1** TGA) (**23**)	53	+3	−93	−259	−12.2
5′-d(TAG GTC **1**AT ACT) (**19**)					
3′-d(ATC CAG TTA TG**1**) (**22**)	51	+1	−84	−233	−11.7
5′-d(TAG GTC **1**AT ACT) (**19**)					
3′-d(ATC C**1**G TT**1** TGA) (**23**)	55	+5	−89	−245	−12.9
5′-d(TAG GTC **11**T ACT) (**20**)					
3′-d(ATC CAG TTA TG**1**) (**22**)	54	+4	−80	−218	−12.3
5′-d(TAG GTC **11**T ACT) (**20**)					
3′-d(ATC C**1**G TT**1** TGA) (**23**)	59	+9	−86	−234	−13.6
5′-d(T**1**G GTC **11**T **1**CT) (**21**)					
3′-d(ATC CAG TTA TG**1**) (**22**)	57	+7	−95	−261	−13.8
5′-d(T**1**G GTC **11**T **1**CT) (**21**)					
3′-d(ATC C**1**G TT**1** TGA) (**23**)	60	+10	−109	−301	−15.5

[a] Measured at 260 nm in 1 M NaCl, 100 mM $MgCl_2$, and 60 mM Na-cacodylate (pH 7.0) with 5 μM + 5 μM single-strand concentration. [b] Refers to the contribution of the modified residues. [c] Thermodynamic values were calculated with the program *MeltWin* 3.0 and are with 10% deviation.

Scheme 3. Synthesis of Nucleoside "Click" Conjugates 12−15

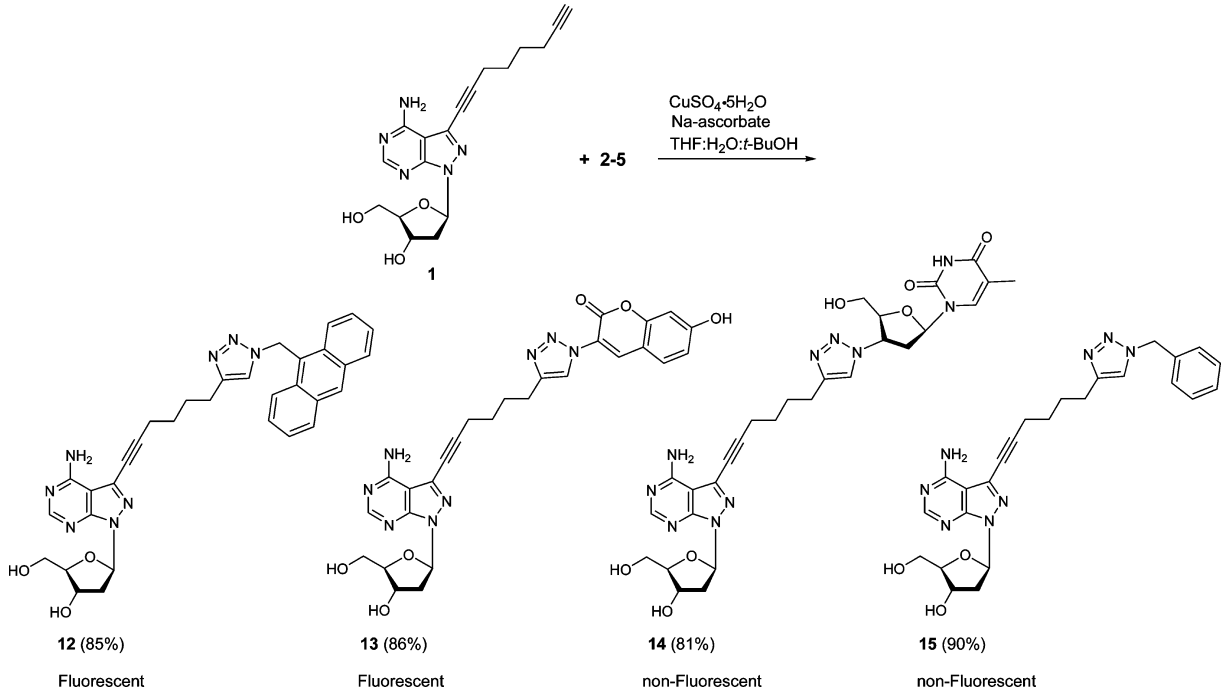

d(TAG GTC AAT ACT) (**17**)·3′-d(ATC CAG TTA TGA) (**18**) is chosen as reference duplex. This standard duplex is further modified at various positions with alkynyl nucleoside **1**. One of the dA residues was replaced at the peripheral position with the alkynyl-modified residue and melting studies have been performed. As is shown in Table 2, this resulted in about 2 °C increase in T_m value per modification (**17**·**22**), whereas incorporation at the central position resulted 1 °C increase (**19**·**18**). Further, the measurements were performed with multiple incorporations at different positions with different numbers. When one strand is modified with two residues keeping the complementary strand unchanged (duplexes **17**·**23** and **20**·**18**), a 3 and 4 °C increase in T_m per modification is observed, respectively. These encouraging results tempted us to modify one strand completely keeping its complementary strand unchanged. T_m measurement result of duplex **21**·**18** showed 6 °C T_m increase. Of note, furthermore modifications (total six modifications in a duplex) were performed resulting in oligonucleotide duplex **21**·**23**, which gave a T_m value 10 °C higher than the unmodified duplex.

"Click" Reaction Performed on 8-Aza-7-deaza-2′-deoxyadenosine Derivative 1 and Properties of Nucleoside Conjugates. The efficacy of the "click" reaction on nucleoside **1** was studied with the two nonfluorescent molecules benzyl azide **4** (nonpolar) and AZT **5** (polar). Then, the cycloaddition was performed also with the fluorogenic dyes 9-azidomethyl anthracene **2** and 3-azido-7-hydroxycoumarin **3** (Scheme 3). We were successfully able to "click" all four azides (**2**−**5**) to nucleoside **1** (to get click conjugates**12**−**15**). The reactions were performed in the presence of $CuSO_4$·$5H_2O$ using sodium

Table 3. ^{13}C NMR Chemical Shifts of the Nucleoside Conjugates[a]

compd	C(2)[b] C(6)[c]	C(4)[b] C(7a)[c]	C(5)[b] C(3a)[c]	C(6)[b] C(4)[c]	C(7)[b] C(3)[c]	C≡C	triazole	ligand CH_2/CH_3
12	156.7	153.6	100.8	157.8	127.3	96.6, 72.1	146.6, 124.0	54.9
13	156.6[d]	156.3[d]	102.1	157.7	127.3	96.5, 72.2	146.8, 122.9	--
14	156.1	153.1	100.3	157.2	126.8	96.0, 71.6	146.4, 120.9	11.7
15	156.7	153.6	100.8	157.8	127.3	96.5, 72.2	146.9, 122.1	52.7
16	152.6	149.0	95.6	157.6	127.1	92.4, 73.7	146.6, 124.1	54.9

compd	C1′	C2′	C3′	C4′	C5′	side chain CH_2/CH_3
12	84.0	37.9	71.0	87.7	62.4	28.3, 27.2, 24.3, 18.6
13	84.0	37.9	70.9	87.7	62.3	28.2, 27.2, 24.3, 18.7
14	83.9	37.3	71.6	87.2	61.8	27.7, 26.7, 24.0, 18.2
15	84.0	37.9	71.0	87.7	62.4	28.4, 27.3, 24.5, 18.7
16	83.1	38.7	71.0	87.5	61.9	28.3, 27.8, 24.4, 18.6

[a] Measured in DMSO-d_6 at 298 K. ^{13}C chemical shifts were unambiguously assigned by gated-decoupled ^{1}H−^{13}C NMR spectra if not otherwise stated. For ^{1}H−^{13}C coupling constants, see Table S2, Supporting Information. [b] Purine numbering. [c] Systematic numbering. [d] Tentative.

ascorbate as a reducing agent in the aqueous media of *t*-BuOH/THF (1:3) at room temperature. The purification of polar residue conjugated nucleosides and oligonucleotides is somewhat difficult as is the case with residues **3** and **5**. As expected, the nucleoside conjugate **14**, which becomes more polar after conjugation through triazole formation, migrates faster than the nucleoside **1** itself (Supporting Information). The more hydrophobic benzyl residue increases the lipophilicity of the conjugate **15** making it more nonpolar. Therefore, it moves more slowly than nucleoside **1**. The HPLC profiles of the conjugates were taken as a reference for the oligonucleotide separation after click reaction.

The "click" conjugates were characterized by ^{1}H and ^{13}C NMR, as well as ^{1}H−^{13}C NMR gated decoupled spectra (for ^{1}H−^{13}C NMR coupling constants, see Supporting Information). Appearance of two new signals at (i) δ = 146.6 and 124.0 ppm (**12**), (ii) δ = 146.8 and 122.9 ppm (**13**), (iii) δ = 146.4 and 120.9 ppm (**14**), and (iv) 146.9 and 122.1 ppm (**15**) (Table 3) and absence of terminal C≡C carbon atom signals in ^{13}C NMR confirms formation of the triazole system where steric hindrance offers no space for bis-functionlization of the second C≡C. The ^{13}C NMR chemical shifts of the side chain for the functionalized dye conjugates are listed in Table 3.

The 7-alkynyl side chain has a decisive influence on the UV−vis spectra of 8-aza-7-deaza-2′-deoxyadenosine (**34**). Already, the nonfunctionalized 8-aza-7-deaza-2′-deoxyadenosine shows a rather different spectrum (Supporting Information) compared to that of 2′-deoxyadenosine (one main maximum at 261 nm); the octadiynyl side chain of derivative **1** induces further changes which are due to the triple bond of the side chain being in conjugation with the heterocyclic moiety. Significant changes occur in the case of click conjugates. Already, the adducts with AZT (**14**) and benzylazide (**15**) change the UV spectra significantly due to the addition of the UV-active ligands and the generation of the 1,2,3-triazole system (Supporting Information). When 3-azidocoumarin **3** or 9-azidomethyl anthracene **2** are clicked to compound **1**, additional UV absorbance emerge in the 300−400 nm region (Supporting Information). For the quantification of the modified oligonucleotides by UV spectroscopy, the extinction coefficients of conjugates were determined at the UV maxima. For spectra and extinction coefficient values, see Supporting Information.

"Click" Reactions Performed on Oligonucleotides Containing Nucleoside 1 and Photophysical Properties of Dye Conjugates. Next, the "click" reaction was performed on oligonucleotide **19** to prove the feasibility of the reaction in a more crowded situation like in DNA (Scheme 4). The reaction was performed at room temperature in aqueous solution of DMSO and *t*-BuOH to yield postsynthetically labeled ODNs. For this, at first the Cu:TBTA ligand complex was prepared by mixing the components in a 1:1 ratio in H_2O/*t*-BuOH (9:1). Then, the alkyne containing oligonucleotide was added. Thereafter, other components like azide, TCEP, and $NaHCO_3$ were added and the reaction mixture was stirred at rt for 12 h. Afterward, the reaction mixture was dried and dissolved in 0.5 mL of water and centrifuged (14 000 rpm) to remove the inorganic salts and insoluble materials. Purification by RP-HPLC led to the modified ODNs. The polytriazole ligand, TBTA, is used to stabilize Cu(I), in the presence of TCEP as a reducing agent. Excess and/or uncomplexed copper led to the strand breaks of the oligonucleotide chain. Hence, it is necessary to add copper and azide in the specified amount. It appears that the click reaction proceeds at different velocities with respect to the particular azide. Nevertheless, kinetic experiments have not been performed. Usually, the click reactions were carried out with 5 A_{260} units of oligonucleotide. For details, see the Experimental Procedures section.

Scheme 4. "Click" Conjugates 27−30 Formed by the Cycloaddition of Oligonucleotide 19 with Azides 2−5

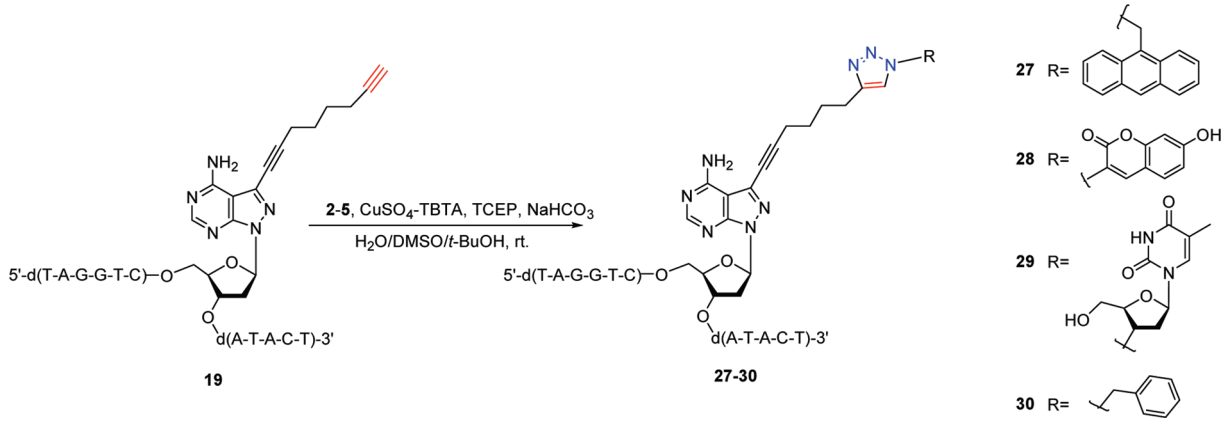

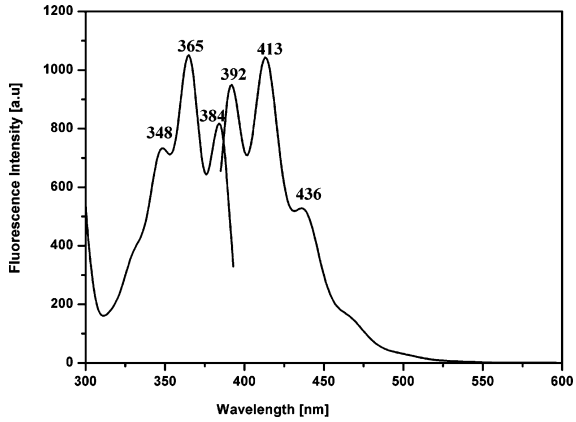

Figure 2. Excitation and emission spectra of the nucleoside anthracene conjugate **12** measured in methanol.

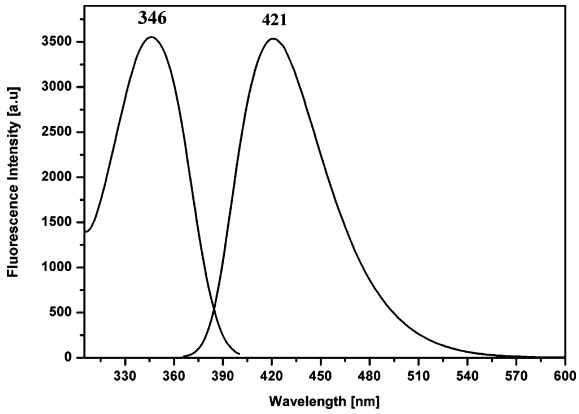

Figure 3. Excitation and emission spectra of the nucleoside coumarin conjugate **13** measured in methanol.

Photoexcitable dyes such as anthracene or coumarin suffer from fluorescence quenching, when conjugated to nucleobases such as purines or 7-deazapurines. The quenching causes problems in the in situ fluorescence hydridization (FISH). The quenching is often unwanted, e.g., in DNA-sequencing with fluorescence dye-labeled terminators or on biochips. However, intramolecular fluorescence quenching is used in dye-labeled molecular beacons. Apart from environmental effects (salt, solvent, etc.), quenching occurs by fluorescence resonance energy transfer (FRET) or charge separation between the dye and a DNA base. In order to evaluate the influence of the 8-aza-7-deazaadenine base, the fluorescence properties of nucleoside conjugates **12** and **13** were investigated and compared. The measurements were performed in methanol (Figures 2 and 3). For solubility reasons, dye conjugates were dissolved in 0.5 mL of DMSO and then diluted with 99.5 mL methanol. In all experiments, the concentration of the nucleoside dye conjugates was identical (0.98 μmol). Conjugate **12** shows the main excitation maximum at 365 nm with an emission maximum at 413 nm (Figure 2). However, nucleoside dye conjugate **13** shows an excitation maximum at 346 nm and emission maximum at 421 nm (Figure 3). While the Stokes shift of the anthracene conjugate is only 48 nm, it amounts to 75 nm in the coumarin conjugate.

To evaluate quenching of the 8-aza-7-deazaadenine moiety within the monomeric anthracene conjugate **12**, fluorescence data of the anthracene conjugate were compared with that of the abasic alkyne side chain conjugate **32**. Similar experiments were performed on the 8-aza-7-deazaadenine coumarin conjugate **13** and the abasic coumarin alkyne derivative **33**. It was anticipated that the octyne side chain conjugated with triazole

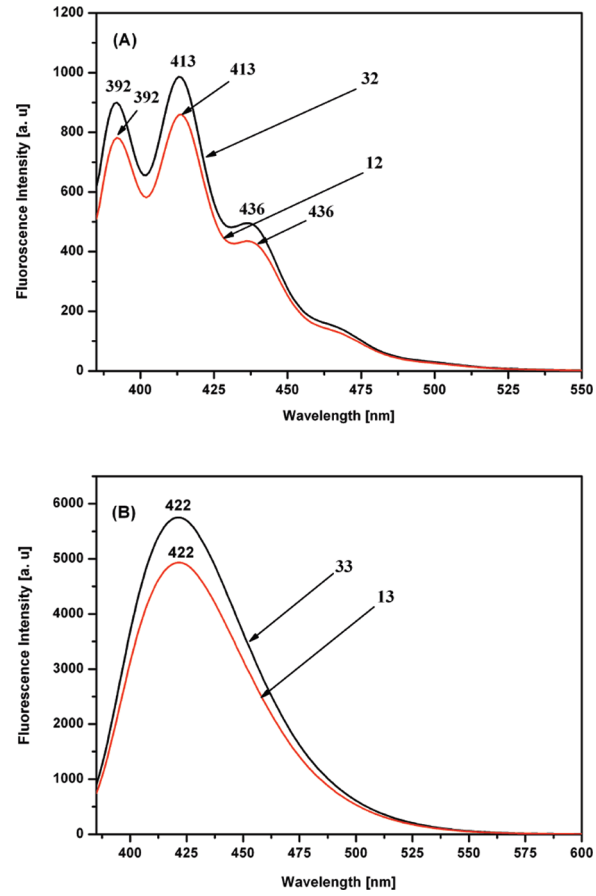

Figure 4. (A) Fluorescence emission spectra of the nucleoside conjugate **12** and the octyne conjugate **32**. (B) Fluorescence emission spectra of the nucleoside conjugate **13** and octyne conjugate **33**. For measurements, identical molar concentrations of the triazole conjugates were used. Spectra were measured in methanol.

Scheme 5. Synthesis of Abasic Click Conjugates

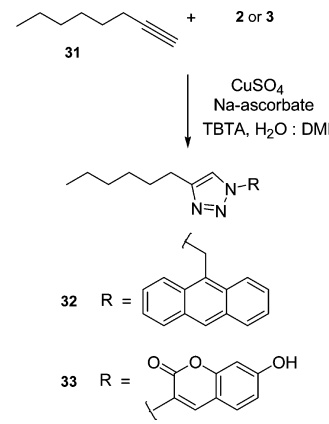

moiety should have no significant influence on the fluorescence of the dye. After clicking the azido dye **2** to the octyne **31**, the formed conjugate was purified by FC and compound **32** was isolated in 91% yield. As shown in Figure 4A,B, both nucleoside conjugates **12** and **13** do not develop significant fluorescence quenching when compared with corresponding abasic octyne derivatives **32** and **33**. So, 8-aza-7-deazaadenine virtually do not quench the fluorescence within the coumarin or anthracene conjugates.

Further, the fluorescence quenching behavior of pyrazolo[3,4-*d*]pyrimidine vs pyrrolo[2,3-*d*]pyrimidine is compared. To evaluate quenching of the 7-deaza-2′-deoxyadenosine within the

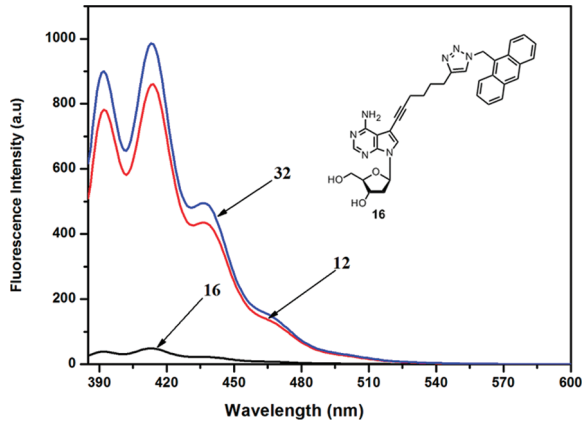

Figure 5. Comparison of fluorescence of anthracene click conjugates **12**, **32**, and **16**. Measurements were performed at identical molar concentration (0.98 μM) in methanol.

anthracene conjugate **16**, the octa-1,7-diynyl nucleoside derivative was functionalized with anthracene azide **2** in a similar way as 8-aza-7-deaza-2′-deoxyadenosine derivative **1**, yielding the conjugate **16** in 78%. When compared, the fluorescence intensity is reduced by around 95%, to that of the pyrazolo[3,4-*d*]pyrimidine conjugate **12** or the abasic anthracene derivative **32** (Figure 5). As in other cases (*14, 33, 36, 37*), quenching within the 7-deazaadenine conjugate **16** is attributed to a charge transfer between the nucleobase and the dye. This results from the low oxidation potentials of 7-deazapurine-2′-deoxyribonucleosides compared to purines. The oxidation potentials against the standard calomel electrode (SCE) decrease in the following order dA (1.39 V) > c^7A_d (1.15 V) > dG (1.07 V) > c^7G (0.74 V) (*38*). The oxidation potential is further influenced by nearest-neighbor bases in single-stranded DNA, by base pairing in duplex DNA and by modification of the base moiety with side chains as in compound **1**. During charge separation, the nucleobase (NB) can be oxidized forming the radical cation, and a dye yields a radical anion ($DYE^{\bullet-} - NB^{\bullet+}$) (*35, 55−57*). Depending on the redox potential of the nucleobase and the dye molecule, the process can be reversed leading to the formation of a dye radical cation and a nucleobase anion ($DYE^{\bullet+} - NB^{\bullet-}$) (*35, 55−57*). Consequently, DNA bases and base surrogates can act in either way according to their redox potentials. The experiments described above clearly evidence that contrary to the 7-deazaadenine moiety—which is attributed to the low oxidation potential of pyrrolo[2,3-*d*]pyrimidine—the 8-aza-7-deazaadenine moiety of the 8-aza-7-deazaadenine conjugate is not able to quench the fluorescence of the dye significantly, most likely due to its higher oxidation potential.

Next, fluorescence measurements were performed on major groove functionalized oligonucleotides. The fluorescence spectra of single-stranded (ss) oligonucleotide 5′-d(TAG GTC **13**AT ACT) (**28**) bearing the coumarin dye shows an excitation maximum at 398 nm and an emission at 478 nm (Figure 6A). The corresponding anthracene conjugate 5′-d(TAG GTC **12**AT ACT) (**27**) shows a strong fluorescence with emission maximum at 424 nm and excitation maximum at 371 nm (Figure 6C). Upon hybridization with the unmodified complementary strand,

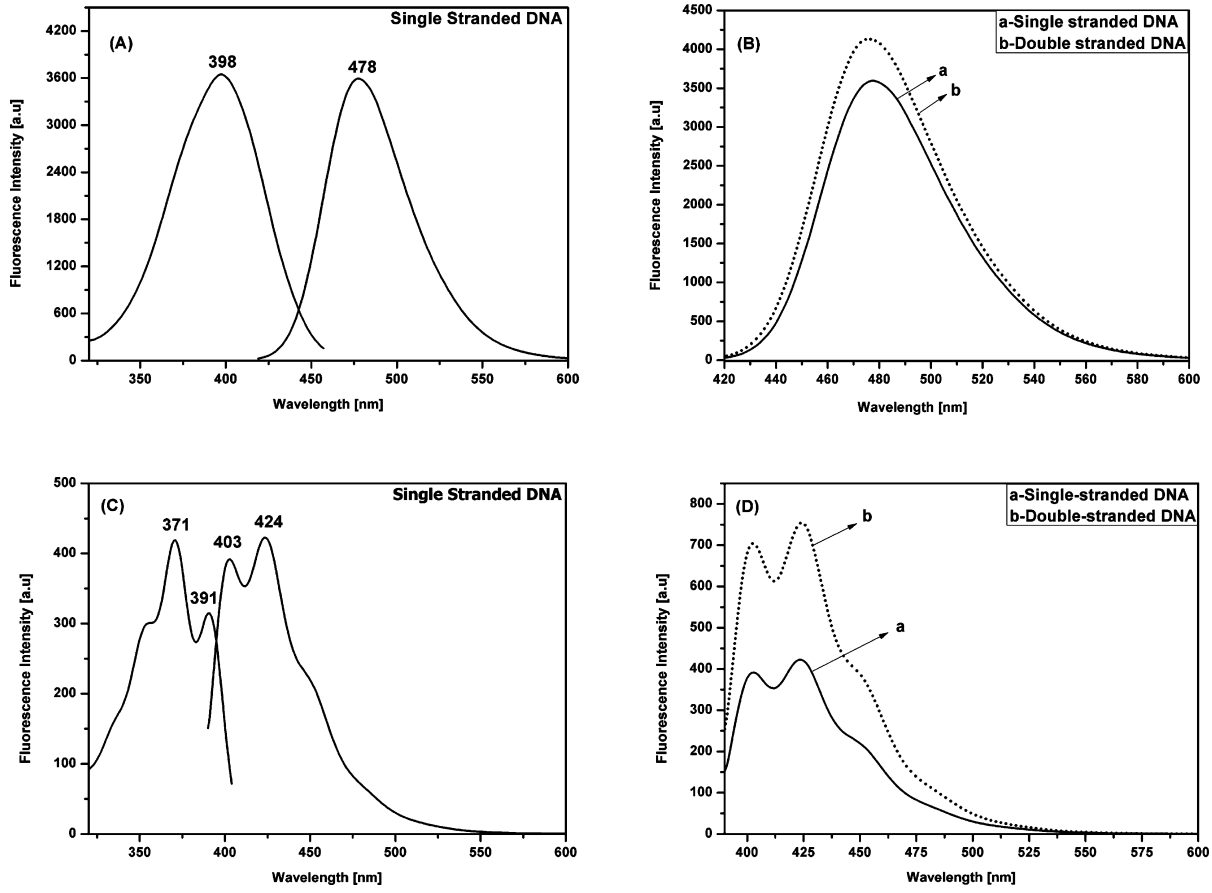

Figure 6. (A) Excitation and emission spectra of the single-stranded oligonucleotide coumarin conjugate **28** (2 μM single-strand concentration). (B) Comparison of the fluorescence emission spectra of the single-stranded oligonucleotide **28** and the duplex **28·18** (2 μM + 2 μM single-strand concentration) when excited at 398 nm. (C) Excitation and emission spectra of the single-stranded oligonucleotide anthracene conjugate **27** (2 μM single-strand concentration). (D) Comparison of the fluorescence emission spectra of the single-stranded oligonucleotide **27** and the duplex **27·18** (2 μM + 2 μM single-strand concentration) when excited at 371 nm. Spectra were measured in 1 M NaCl, 100 mM $MgCl_2$, 60 mM Na-cacodylate buffer at pH = 8.5.

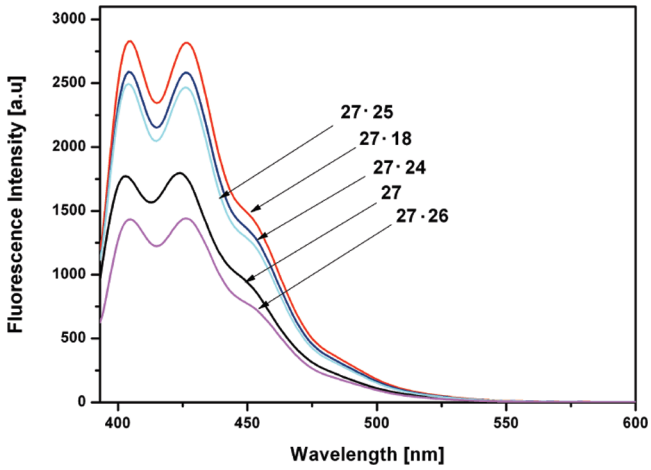

Figure 7. Fluorescence spectra of oligonucleotide duplexes **27·18**, **27·25**, **27·24**, and **27·26** containing the anthracene conjugate **12** and single-stranded oligonucleotide **27**. For oligonucleotide sequences, see Table 4. Measurements were performed in 1 M NaCl, 100 mM $MgCl_2$, and 60 mM Na-cacodylate (pH 7.0) with 5 μM + 5 μM single-strand concentration.

the duplexes 5′-d(TAG GTC **12**AT ACT) (**27**)·3′-d(ATC CAG TTA TGA) (**18**) and 5′-d(TAG GTC **13**AT ACT) (**28**)·3′-d(ATC CAG TTA TGA) (**18**) were formed, where in both cases the dye residue is located at the center of ODN. In case of duplex **27·18**, fluorescence intensity is significantly increased by almost a factor of 2 (ss vs ds) from single strand to duplex (Figure 6D), whereas only a small fluorescence increase is observed during duplex formation of the oligonucleotide coumarin conjugate (ODNs ss **28** and ds **28·18**, viz., 3590 vs 4130 fluorescence intensity; Figure 6B), which is contrary to that of the related pyrrolo[2,3-*d*]pyrimidine oligonucleotide coumarin conjugates (*14, 18*).

The strong fluorescence increase upon duplex formation observed for the oligonucleotide anthracene conjugate prompted us to evaluate the potential of fluorescence change for single-base mismatch discrimination. A set of the single-stranded oligonucleotides **24**−**26** was synthesized and hybridized with a complementary strand containing anthracene conjugate **12** generating a duplex with fully matched base pairs and three duplexes with mismatches at the center of the oligonucleotide duplex. As mentioned earlier, the fluorescence intensity of the fully matched duplex (**27·18**) is the highest, while that with the **12**-dC mismatch (**27·26**) is the lowest. The **12**-dA and **12**-dG mismatches (**27·24** and **27·25**) show similar fluorescence intensity (Figure 7). From this, we can conclude that an anthracene "click" conjugate linked to fully matched base pairs can be distinguished from a mismatch situation. However, as observed in many other cases, it is difficult to differentiate among the various mismatched base pairs. We anticipate that the anthracene moiety interacts with distant base pairs one or two positions away from the site of the mismatch, a situation which does not lead to extreme changes of the dye fluorescence.

Furthermore, the stabilities of the fully matched and mismatched duplexes were measured and compared. The anthracene residue leads to a tremendous increase in stability (ΔT_m 9 °C per modification) in fully matched and mismatched duplexes (Table 4). The fully matched duplex **27·18** displays the highest melting temperature (59 °C) and also displays the maximum fluorescence intensity compared to the counterpart mismatched duplexes. The duplexes with mismatches are significantly less stable (ΔT_m −11 to −15 °C). The duplex with the mismatched base dC gives the lowest T_m value (43 °C), which also exhibits the lowest fluorescence intensity among the mismatched duplexes. Nevertheless, duplexes with mismatches bearing anthracene are almost as stable as the unmodified duplex **17·18**. To shed more light into this matter, the mismatch discrimination was studied in the unmodified duplexes. Almost similar T_m decreases (−12 to 16 °C) are observed as for the duplexes containing the anthracene conjugate but with a value always approximately 9 °C lower than those of the modified ones (Table 4). This implies that the anthracene moiety is always interacting with the same base pair, most likely one or two positions away from the mismatch site. To model this situation, energy minimization calculations using Amber MM+ force field (*Hyperchem 7.0/8.0*; Hypercube Inc., Gainesville, FL, USA, 2001) were performed on the 12-mer duplexes **27·18**, **28·18**, and **29·18**, taking B-type DNA in account.

Table 4. T_m Values and Thermodynamic Data of Oligonucleotide Duplexes Containing Mismatches

duplexes	T_m[a] [°C]	ΔT_m[b] [°C]	$\Delta H°$[c] [kcal/mol]	$\Delta S°$ [cal/(mol K)]	$\Delta G°_{310}$ [kcal/mol]
5′-d(TAG GTC **12**AT ACT) (**27**)					
3′-d(ATC CAG **T**TA TGA) (**18**)	59	0	−85	−230	−13.7
5′-d(TAG GTC **12**AT ACT) (**27**)					
3′-d(ATC CAG **A**TA TGA) (**24**)	44	−15	−69	−193	−9.6
5′-d(TAG GTC **12**AT ACT) (**27**)					
3′-d(ATC CAG **G**TA TGA) (**25**)	47	−12	−74	−206	−10.2
5′-d(TAG GTC **12**AT ACT) (**27**)					
3′-d(ATC CAG **C**TA TGA) (**26**)	43	−16	−70	−196	−9.4
5′-d(TAG GTC **A**AT ACT) (**17**)					
3′-d(ATC CAG **T**TA TGA) (**18**)	50	0	−89	−249	−11.6
5′-d(TAG GTC **A**AT ACT) (**17**)					
3′-d(ATC CAG **A**TA TGA) (**24**)	38	−12	−63	−178	−8.2
5′-d(TAG GTC **A**AT ACT) (**17**)					
3′-d(ATC CAG **G**TA TGA) (**25**)	39	−11	−68	−193	−8.3
5′-d(TAG GTC **A**AT ACT) (**17**)					
3′-d(ATC CAG **C**TA TGA) (**26**)	35	−15	−73	−212	−7.6

[a] Measured at 260 nm in 1 M NaCl, 100 mM $MgCl_2$, and 60 mM Na-cacodylate (pH 7.0) with 5 μM + 5 μM single-strand concentration. [b] Refers to the contribution of the modified residues. [c] Thermodynamic values were calculated with the program *MeltWin 3.0* and are with 10% deviation.

Table 5. T_m Values and Thermodynamic Data of Oligonucleotide Duplexes Containing Nucleosides 12−15

duplexes	T_m[a] [°C]	ΔT_m[b] [°C]	$\Delta H°$[c] [kcal/mol]	$\Delta S°$ [cal/(mol K)]	$\Delta G°_{310}$ [kcal/mol]
5′-d(TAG GTC AAT ACT) (**17**)					
3′-d(ATC CAG TTA TGA) (**18**)	50	--	−89	−249	−11.6
5′-d(TAG GTC **12**AT ACT) (**27**)					
3′-d(ATC CAG TTA TGA) (**18**)	59	+9	−85	−230	−13.7
5′-d(TAG GTC **13**AT ACT) (**28**)					
3′-d(ATC CAG TTA TGA) (**18**)	50	0	−82	−229	−11.2
5′-d(TAG GTC **14**AT ACT) (**29**)					
3′-d(ATC CAG TTA TGA) (**18**)	51	+1	−94	−275	−12.0
5′-d(TAG GTC **15**AT ACT) (**30**)					
3′-d(ATC CAG TTA TGA) (**18**)	51	+1	−82	−226	−12.4

[a] Measured at 260 nm in 1 M NaCl, 100 mM $MgCl_2$, and 60 mM Na-cacodylate (pH 7.0) with 5 μM + 5 μM single-strand concentration. [b] Refers to the contribution of the modified residues. [c] Thermodynamic values were calculated with the program *MeltWin 3.0* and are with 10% deviation.

Duplex Stability of Oligonucleotide Conjugates and Molecular Dynamics Calculations. Next, stability of the duplexes formed with complementary strands by "click" functionalized oligonucleotides was investigated. For this, T_m measurements were performed. As shown in Table 5, the coumarin dye conjugate **13** exerts no significant influence on the stability of duplex **28·18**, while the AZT and benzyl conjugates slightly stabilize the DNA duplex. A T_m value increase of 1 °C in both cases was observed, indicating positive interactions between these residues within duplex DNA. A significant stabilization (+9 °C) is observed in duplex **27·18** bearing an anthracenyl side chain. We think that the anthracene residue intercalates to proximal DNA bases (*58*). The strong

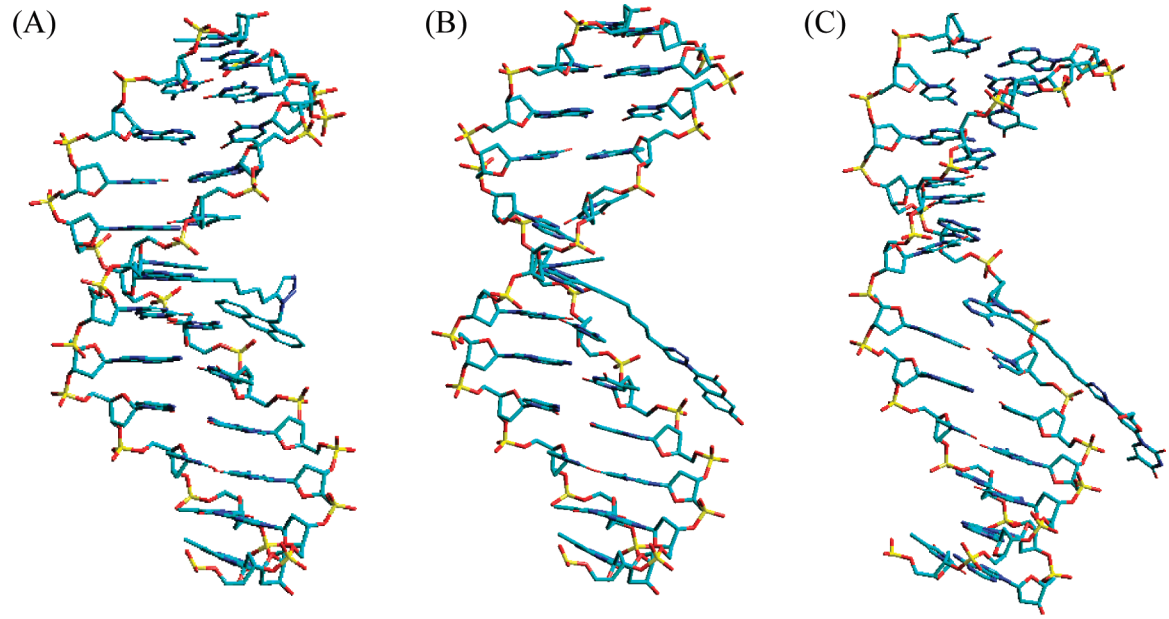

Figure 8. Molecular dynamics (MD) simulation models of oligonucleotide duplexes. The models were constructed using *Hyperchem 8.0* and energy minimized using AMBER calculations. (A) Oligonucleotide duplex **27·18** with an octa-1,7-diynyl side chain modified with anthracene azide. (B) Duplex **28·18** with an octadiynyl side chain modified with coumarin azide. (C) Duplex **29 ·18** with an octadiynyl chain modified with AZT. For a better view, structure (C) was rotated counter-clockwise.

hydrophobic interaction arising due to anthracene π-system, as a major binding mode with the DNA bases, results in an intercalated anthracene probe (*59*). The contribution of methylene groups present in the octa-1,7-diyinyl side chain toward free energy is substantial (*60*). Combined effect of these factors stabilizes the DNA helix (duplex **27·18**) to a significant extent with concomitant increase in melting temperature (+9 °C) compared to duplex **17·18**.

Next, energy minimization calculations were performed. According to Figure 8, back-folding of the side chain and possible π-stacking of the anthracene residue is supported by energy minimization. We do not see the intercalation of the anthracene residue with the mentioned program, while the polar, negatively charged coumarin fluorophore protrudes into the more polar environment. Both bulky residues are accommodated well in the B-DNA duplex.

CONCLUSIONS

Oligonucleotides incorporating octa-(1,7)-diynyl-8-aza-7-deaza-2′-deoxyadenosine **1** were prepared and further functionalized by azide−alkyne Huisgen-Meldal-Sharpless cycloaddition ("click" reaction), on both nucleoside and oligonucleotide level. The nonfluorescent fluorogenic reporter groups led to the formation of highly fluorescent dye conjugates after click reaction. The anthracene dye conjugate, which acts as a strong DNA binding ligand, pronounces the stability of a DNA duplex by 9 °C by a single modification. This results from anticipated intercalation of the dye and the hydrophobic interaction of the side chain. The 8-aza-7-deaza-2′-deoxyadenosine dye conjugates **12** and **13** show almost no fluorescence quenching, whereas the fluorescence is strongly quenched in the case of the 7-deazaadenine counterpart **16**. Quenching was also studied with the 1-octyne click conjugates taking both fluorogenic and polar as well as nonpolar dyes **2** and **3**. The fluorescence of single-stranded dye conjugates is increased upon duplex formation. A fully matched duplex shows a higher fluorescence than those with mismatches formed with dA, dG, and dC located opposite compound **1**, which also shows the highest T_m value. Thus, the 8-aza-7-deaza-2′-deoxyadenosine is an ideal shape mimic of 2′-deoxyadenosine, allowing functionalization at the 7-position without disturbing the DNA helix structure, which was supported by molecular dynamics simulations. It generates virtually no fluorescence quenching by charge transfer as observed for 7-deazaadenine conjugates.

ACKNOWLEDGMENT

We would like to thank Dr. V. R. Sirivolu, Dr. P. Chittepu, and Dr. P. Leonard for helpful discussions and support. We also thank Dr. S. Budow and Mr. D. Jiang for measuring the NMR spectra, Dr. T. Koch from Roche Diagnostics GmbH, Penzberg, Germany, for the measurement of the MALDI spectra, and Mr. Nhat Quang Tran for the oligonucleotide syntheses. Financial support by the Roche Diagnostics GmbH and ChemBiotech, Muenster, Germany, is highly appreciated.

Supporting Information Available: $^{1}H-^{13}C$ NMR coupling constants, extinction coefficients, HPLC profiles, MALDI-TOF masses and purification profiles of the oligonucleotides, melting profiles, ^{1}H and ^{13}C NMR spectra of the nucleoside derivatives and click conjugates. This material is available free of charge via the Internet at http://pubs.acs.org.

LITERATURE CITED

(1) Kobayashi, H., Ogawa, M., Alford, R., Choyke, P. L., and Urano, Y. (2010) New strategies for fluorescent probe design in medical diagnostic imaging. *Chem. Rev.* DOI: 10.1021/cr900263j.

(2) Hrdlicka, P. J., Babu, B. R., Sørensen, M. D., Harrit, N., and Wengel, J. (2005) Multilabeled pyrene-functionalized 2′-amino-LNA probes for nucleic acid detection in homogeneous fluorescence assays. *J. Am. Chem. Soc. 127*, 13293–13299.

(3) Astakhova, I. V., Korshun, V. A., Jahn, K., Kjems, J., and Wengel, J. (2008) Perylene attached to 2′-amino-LNA: Synthesis, incorporation into oligonucleotides, and remarkable fluorescence properties *in vitro* and in cell culture. *Bioconjugate Chem. 19*, 1995–2007.

(4) Marti, A. A., Jockusch, S., Stevens, N., Ju, J., and Turro, N. J. (2007) Fluorescent hybridization probes for sensitive and selective DNA and RNA detection. *Acc. Chem. Res. 40*, 402–409.

(5) Hakala, H., and Lönnberg, H. (1997) Time-resolved fluorescence detection of oligonucleotide hybridization on a single microparticle: Covalent immobilization of oligonucleotides and quantitation of a model system. *Bioconjugate Chem. 8*, 232–237.

(6) Cuppoletti, A., Cho, Y., Park, J.-S., Strässler, C., and Kool, E. T. (2005) Oligomeric fluorescent labels for DNA. *Bioconjugate Chem. 16*, 528–534.

(7) Droumaguet, C. L., Wang, C., and Wang, Q. (2010) Fluorogenic click reaction. *Chem. Soc. Rev.* DOI: 10.1039/b901975h.

(8) Best, M. D. (2009) Click chemistry and bioorthogonal reactions: Unprecedented selectivity in the labeling of biological molecules. *Biochemistry 48*, 6571–6584.

(9) Huisgen, R. (1989) Kinetics and reaction mechanisms: Selected examples from the experience of forty years. *Pure Appl. Chem. 61*, 613–628.

(10) Huisgen, R., Szeimies, G., and Moebius, L. (1967) Kinetik der Additionen organischer Azide an CC-Mehrfachbindungen. *Chem. Ber. 100*, 2494–2507.

(11) Meldal, M., and Tornøe, C. W. (2008) Cu-catalyzed azide-alkyne cycloaddition. *Chem. Rev. 108*, 2952–3015.

(12) Tornøe, C. W., Christensen, C., and Meldal, M. (2002) Peptidotriazoles on solid phase: [1,2,3]-Triazoles by regiospecific copper(I)-catalyzed 1,3- dipolar cycloadditions of terminal alkynes to azides. *J. Org. Chem. 67*, 3057–3064.

(13) Rostovtsev, V. V., Green, L. G., Fokin, V. V., and Sharpless, K. B. (2002) A stepwise Huisgen cycloaddition process: Copper (I)-catalyzed regioselective "ligation" of azides and terminal alkynes. *Angew. Chem., Int. Ed. 41*, 2596–2599.

(14) Seela, F., Sirivolu, V. R., and Chittepu, P. (2008) Modification of DNA with octadiynyl side chains: Synthesis, base pairing, and formation of fluorescent coumarin dye conjugates of four nucleobases by the alkyne-azide "click" reaction. *Bioconjugate Chem. 19*, 211–224.

(15) Gramlich, P. M. E., Wirges, C. T., Manetto, A., and Carell, T. (2008) Postsynthetic DNA modification through the copper-catalyzed azide-alkyne cycloaddition reaction. *Angew. Chem., Int. Ed. 47*, 8350–8358.

(16) Kocalka, P., El-Sagheer, A. H., and Brown, T. (2008) Rapid and efficient DNA strand cross-linking by click chemistry. *ChemBioChem 9*, 1280–1285.

(17) Hotha, S., and Kashyap, S. (2006) "Click chemistry" inspired synthesis of *pseudo*-oligosaccharides and amino acid glycoconjugates. *J. Org. Chem. 71*, 364–367.

(18) Seela, F., Xiong, H., Leonard, P., and Budow, S. (2009) 8-Aza-7-deazaguanine nucleosides and oligonucleotides with octadiynyl side chains: Synthesis, functionalization by the azide-alkyne 'click' reaction and nucleobase specific fluorescence quenching of coumarin dye conjugates. *Org. Biomol. Chem. 7*, 1374–1387.

(19) Sirivolu, V. R., Chittepu, P., and Seela, F. (2008) DNA with branched internal side chains: Synthesis of 5-tripropargylamine-dU and conjugation by an azide-alkyne double click reaction. *ChemBioChem 9*, 2305–2316.

(20) Agnew, B., Buck, S., Nyberg, T., Bradford, J., Clarke, S., and Gee, K. (2008) Click chemistry for labeling and detection of biomolecules. Molecular probes for biomedical applications II; 21−22 January 2008, San Jose, CA, USA; 6867, 1−686708−10.

(21) Baskin, J. M., Prescher, J. A., Laughlin, S. T., Agard, N. J., Chang, P. V., Miller, I. A., Lo, A., Codelli, J. A., and Bertozzi, C. R. (2007) Copper-free click chemistry for dynamic in vivo imaging. *Proc. Natl. Acad. Sci. U.S.A. 104*, 16793–16797.

(22) Froehler, B. C., Wadwani, S., Terhorst, T. J., and Gerrard, S. R. (1992) Oligodeoxynucleotides containing C-5 propyne analogs of 2′-deoxyuridine and 2′-deoxycytidine. *Tetrahedron Lett. 33*, 5307–5310.

(23) Graham, D., Parkinson, J. A., and Brown, T. (1998) DNA duplexes stabilized by modified monomer residues: Synthesis and stability. *J. Chem. Soc., Perkin Trans. 1*, 1131–1138.

(24) Sági, J., Szemzö, A., Ébinger, K., Szabolcs, A., Sági, G., Ruff, É., and Ötvös, L. (1993) Base-modified oligodeoxynucleotides. I: Effect of 5-alkyl, 5-(1-alkenyl) and 5-(1-alkynyl) substitution of the pyrimidines on duplex stability and hydrophobicity. *Tetrahedron Lett. 34*, 2191–2194.

(25) Kottysch, T., Ahlborn, C., Brotzel, F., and Richert, C. (2004) Stabilizing or destabilizing oligodeoxynucleotide duplexes containing single 2′-deoxyuridine residues with 5-alkynyl substituents. *Chem.—Eur. J. 10*, 4017–4028.

(26) Seela, F., Zulauf, M., and Debelak, H. (2000) Base-pairing properties of 8-aza-7-deazaadenine linked via the 8-position to the DNA backbone. *Helv. Chim. Acta 83*, 1437–1453.

(27) Seela, F., and Debelak, H. (2001) 8-Aza-7-deazaadenine and 7-deazaguanine: Synthesis and properties of nucleosides and oligonucleotides with nucleobases linked at position-8. *Nucleosides, Nucleotides Nucleic Acids 20*, 577–585.

(28) Seela, F., Zulauf, M., Sauer, M., and Deimel, M. (2000) 7-Substituted 7-deaza-2′-deoxyadenosines and 8-aza-7-deaza-2′-deoxyadenosines: Fluorescence of DNA base analogues induced by the 7-alkynyl side chain. *Helv. Chim. Acta 83*, 910–927.

(29) Seela, F., and Zulauf, M. (1998) Synthesis of 7-alkynylated 8-aza-7-deaza-2′-deoxy adenosines via the Pd-catalysed cross-coupling reaction. *J. Chem. Soc., Perkin Trans. 1*, 3233–3239.

(30) He, J., and Seela, F. (2002) 8-Aza-7-deazapurine-pyrimidine base pairs: The contribution of 2- and 7-substituents to the stability of duplex DNA. *Tetrahedron 58*, 4535–4542.

(31) He, J., and Seela, F. (2002) Propynyl groups in duplex DNA: Stability of base pairs incorporating 7-substituted 8-aza-7-deazapurines or 5-substituted pyrimidines. *Nucleic Acids Res. 30*, 5485–5496.

(32) Seela, F., Jawalekar, A. M., Sun, L., and Leonard, P. (2005) Oligonucleotides containing pyrazolo[3,4-d]pyrimidines: 8-Aza-7-deazaadenines with bulky substituents in the 2- or 7-position. *Nucleosides, Nucleotides Nucleic Acids 24*, 1485–1505.

(33) Wagenknecht, H.-A. (2006) *Charge Transfer in DNA*. Published by Wiley-VCH Verlag GmbH & Co. DOI: 10.1002/3527606629.

(34) Latimer, L. J. P., and Lee, J. S. (1991) Ethidium Bromide does not fluoresce when intercalated adjacent to 7-deazaguanine in duplex DNA. *J. Biol. Chem. 266*, 13849–13851.

(35) Li, H., Peng, X., and Seela, F. (2004) Fluorescence quenching of parallel-stranded DNA bound ethidium bromide: The effect of 7-deaza-2′-deoxyisoguanosine and 7-halogenated derivatives. *Bioorg. Med. Chem. Lett. 14*, 6031–6034.

(36) Genereux, J. C., and Barton, J. K. (2010) Mechanisms for DNA charge transport. *Chem. Rev.* DOI:10.1021/cr900228f.

(37) Seela, F., and Ingale, S. A. (2010) "Double Click" reaction on 7-deazaguanine DNA: Synthesis and excimer fluorescence of nucleosides and oligonucleotides with branched side chains decorated with proximal pyrenes. *J. Org. Chem. 75*, 284–295.

(38) Seidel, C. A. M., Schulz, A., and Sauer, M. H. M. (1996) Nucleobase-specific quenching of fluorescent dyes. 1. Nucleobase one-electron redox potentials and their correlation with static and dynamic quenching efficiencies. *J. Phys. Chem. 100*, 5541–5553.

(39) Cosyn, L., Palaniappan, K. K., Kim, S.-K., Duong, H. T., Gao, Z.-G., Jacobson, K. A., and Van Calenbergh, S. (2006) 2-Triazole-substituted adenosines: A new class of selective A_3 adenosine receptor agonists, partial agonists, and antagonists. *J. Med. Chem. 49*, 7373–7383.

(40) Gierlich, J., Burley, G. A., Gramlich, P. M. E., Hammond, D. M., and Carell, T. (2006) Click chemistry as a reliable method for the high-density postsynthetic functionalization of alkyne-modified DNA. *Org. Lett. 17*, 3639–3642.

(41) Seo, T. S., Li, Z., Ruparel, H., and Ju, J. (2003) Click chemistry to construct fluorescent oligonucleotides for DNA sequencing. *J. Org. Chem. 68*, 609–612.

(42) Hainke, S., and Seitz, O. (2009) Binaphthyl-DNA: Stacking and fluorescence of a nonplanar aromatic base surrogate in DNA. *Angew. Chem., Int. Ed. 48*, 8250–8253.

(43) Dose, C., and Seitz, O. (2008) Single nucleotide specific detection of DNA by native chemical ligation of fluorescence labeled PNA-probes. *Bioorg. Med. Chem. 16*, 65–77.

(44) Chang, K.-C., Su, I.-H., Senthilvelan, A., and Chung, W.-S. (2007) Triazole-modified calix[4]crown as a novel fluorescent on-off switchable chemosensor. *Org. Lett. 9*, 3363–3366.

(45) Stack, D. E., Hill, A. L., Diffendaffer, C. B., and Burns, N. M. (2002) Synthesis of a new fluorescent probe specific for catechols. *Org. Lett. 4*, 4487–4490.

(46) Xie, F., Sivakumar, K., Zeng, Q., Bruckman, M. A., Hodges, B., and Wang, Q. (2008) A fluorogenic 'click' reaction of azidoanthracene derivatives. *Tetrahedron 64*, 2906–2914.

(47) Sivakumar, K., Xie, F., Cash, B. M., Long, S., Barnhill, H. N., and Wang, Q. (2004) A fluorogenic 1,3-dipolar cycloaddition reaction of 3-azidocoumarins and acetylenes. *Org. Lett. 6*, 4603–4606.

(48) Franzini, R. M., and Kool, E. T. (2008) 7-Azidomethoxycoumarins as profluorophores for templated nucleic acid detection. *ChemBioChem 9*, 2981–2988.

(49) Seela, F., and Sirivolu, V. R. (2007) Nucleosides and oligonucleotides with diynyl side chains: The Huisgen-Sharpless cycloaddition "click"reaction" performed on DNA and their constitutents. *Nucleosides, Nucleotides Nucleic Acids 26*, 597–601.

(50) Seela, F., and Zulauf, M. (1999) Oligonucleotides containing 7-deazaadenines: The influence of the 7-substituent chain length and charge on the duplex stability. *Helv. Chim. Acta 82*, 1878–1898.

(51) Becher, G., He, J., and Seela, F. (2001) Major-groove-halogenated DNA: The effects of bromo and iodo substituents replacing H-C(7) of 8-aza-7-deazapurine-2,6-diamine or H-C(5) of uracil residues. *Helv. Chim. Acta 84*, 1048–1065.

(52) Seela, F., and Becher, G. (1999) Oligonucleotides containing pyrazolo[3,4-d]pyrimidines: The influence of 7-substituted 8-aza-7-deaza-2′-deoxyguanosines on the duplex structure and stability. *Helv. Chim. Acta 82*, 1640–1655.

(53) Seela, F., and Becher, G. (2001) Pyrazolo[3,4-d]pyrimidine nucleic acids: Adjustment of dA-dT to dG-dC base pair stability. *Nucleic Acids Res. 29*, 2069–2078.

(54) Seela, F., and Shaikh, K. I. (2005) Oligonucleotides containing 7-propynyl-7-deazaguanine: Synthesis and base pair stability. *Tetrahedron 61*, 2675–2681.

(55) Wagenknecht, H.-A. (2006) DNA as functional π-system: Electron transfer in synthetically modified oligonucleotides. *Functional Organic Materials - Synthesis, strategies, and applications* (Bunz, U. F., and Müller, T. T. J., Eds) pp 441−464, Wiley-VCH, Weinheim, Germany.

(56) Wagenknecht, H.-A. (2006) Electron transfer processes in DNA: Mechanisms, biological relevance and applications in DNA analytics. *Nat. Prod. Rep. 23*, 973–1006.

(57) Wagenknecht, H.-A. (2003) Reductive electron transfer and excess electron migration in DNA. *Angew. Chem., Int. Ed. 42*, 2454–2460.

(58) Wilson, W. D., Wang, Y.-H., Kusuma, S., Chandrasekaran, S., Yang, N. C., and Boykin, D. W. (1985) Binding strength and specificity in DNA interactions: The design of A•T specific intercalators. *J. Am. Chem. Soc. 107*, 4989–4995.

(59) Kumar, C. V., and Asuncion, E. H. (1993) DNA binding studies and site selective fluorescence sensitization of an anthryl probe. *J. Am. Chem. Soc. 115*, 8547–8553.

(60) Duff, M. R., Jr., Mudhivarthi, V. K., and Kumar, C. V. (2009) Rational design of anthracene-based DNA binders. *J. Phys. Chem. B 113*, 1710–1721.

BC100090Y